Mamady KEBE

DESIGN AND FABRICATION OF INTEGRATED INDUCTORS WITH POLYMER-FERROMAGNETIC CORE

M.S.
2014

FATİH UNIVERSITY

The Graduate School of Sciences and Engineering

Master of Science in
Electrical and Electronics Engineering

DESIGN AND FABRICATION OF INTEGRATED INDUCTORS WITH POLYMER-FERROMAGNETIC CORE

by

Mamady KEBE

August 2014

DESIGN AND FABRICATION OF INTEGRATED INDUCTORS WITH POLYMER-FERROMAGNETIC CORE

by

Mamady KEBE

A thesis submitted to

the Graduate School of Sciences and Engineering

of

Fatih University

in partial fulfillment of the requirements for the degree of

Master of Science

in

Electrical and Electronics Engineering

August 2014
Istanbul, Turkey

APPROVAL PAGE

This is to certify that I have read this thesis written by Mamady KEBE and that in my opinion it is fully adequate, in scope and quality, as a thesis for the degree of Master of Science in Electrical and Electronics Engineering.

_____
Asst. Prof. Hüseyin SAĞKOL
Thesis Supervisor

I certify that this thesis satisfies all the requirements as a thesis for the degree of Master of Science in Electrical and Electronics Engineering.

_____
Prof. Dr. Onur TOKER
Head of Department

Examining Committee Members

Asst. Prof. Dr. Hüseyin SAĞKOL _____

Assoc. Prof. Dr. Erdal KORKMAZ _____

Assoc. Prof. Dr. Abdülhadi BAYKAL _____

It is approved that this thesis has been written in compliance with the formatting rules laid down by the Graduate School of Sciences and Engineering.

_____
Assoc. Prof. Dr.Nurullah ARSLAN
Director

August 2014

DESIGN AND FABRICATION OF INTEGRATED INDUCTORS WITH POLYMER-FERROMAGNETIC CORE

Mamady KEBE

M.S. Thesis – Electrical and Electronics Engineering
June 2014

Thesis Supervisor: Asst. Prof. Dr. Hüseyin SAĞKOL

ABSTRACT

The wireless communication system is rapidly improving with the integration of several Integrated Circuits (Ics) on a single chip. This can be observed from devices such as phones and computers which are bearing more and more functions. These devices are composed of many ICs interconnected as a system. Each IC is composed of passive and active elements. The integration of elements such as resistors, transistors and capacitors was overcome without many difficulties. However, the integration of high quality inductors at microwave frequencies still remains a big threat in scaling down remote communication devices.

High inductance inductors require large spacing and usually have smaller operating frequency range. Indeed, scientific researches are being carried on in order to solve these issues. Techniques such as ground shielding, stacking the inductor are imployed to augment the quality factor (Q-Factor) of the inductor. However, implemented inductors using these techniques cannot operate over 5 GHz in general. Further method implicates the use of Ferromagnetic (FM) cores under the spirals of an inductor to enhance its inductance density. This technique takes the advantage of the high permeability of FM nanoparticles. Nevertheless, their high conductivity is a factor of strong eddy currents induction, hence a lower Q-factor inductor is produced. Polymers such as SU-8 have very high resistivity. For instance, the mixture of polymers and FM nanoparticles has a certain value of permeability higher than unity. In addition, it has a high resistivity which can reduce the eddy current losses. Hence, we can use this mixture between the tracks of the spiral inductor. In this manner, we can profit not only from the inductance enhancement due to the high permeability of the FM material but also significant loss reduction due to the high resistivity of the polymer

The methods employed to execute this perspective are practical and the fabrication devices are available. We are aiming to show the improvement of performance after using a mixture of a polymer (SU8) and Ferromagnetic materials in the trenches of a spiral inductor. We will therefore design two types of inductors: one

type uses SU8 and the other type uses FM-SU8 core. Lastly, we will compare the results of the two types of inductors. The microfabrication process includes photolithography of photoresist and SU8, sputtering, lift-off and electroless-plating

Keywords: Q-factor, Inductance density, FM-polymer core, aspect ratio, permeability.

TASARIM VE ENTEGRE İMALAT POLİMER VE FERROMANYETİK ÇEKİRDEK İLE İNDÜKTÖRLERİ

Mamady KEBE

Yüksek Lisans Tezi – Elektrik ve Elektronik Mühendisliği
Haziran 2014

Tez Danışmanı: Asst. Prof. Dr. Hüseyin SAĞKOL

ÖZ

Kablosuz iletişim sistemi hızla tek bir yonga üzerinde çeşitli Entegre Devreler (ICS) entegrasyonu ile geliştirmektedir. Bu tür telefonlar ve daha fazla işlevleri taşıyan bilgisayarlar gibi cihazlardan görülebilir. Bu cihazlar, bir sistem olarak birbirine bağlı çok sayıda IC oluşmaktadır. Her IC aktif ve pasif elemanlardan oluşmaktadır. Bu tür dirençler, transistörler ve kapasitörler gibi elemanların entegrasyonu birçok zorluklar olmadan üstesinden edildi. Ancak, mikrodalga frekanslarında yüksek kaliteli endüktörlerin entegrasyonu hala uzak haberleşme cihazları aşağı ölçeklendirme büyük bir tehdit olmaya devam etmektedir.

Yüksek indüktans endüktörlerde büyük boşluk gerektiren ve genellikle küçük bir çalışma frekansı aralığı vardır. Gerçekten de, bilimsel araştırmalar bu sorunları çözmek amacıyla devam edilmektedir. Bu indüktör istifleme zemin koruyucu gibi teknikler indüktörün kalite faktörü (Q-faktör) artırmak için kullanılmıştır. Ancak, bu teknikler kullanılarak uygulanan endüktörlerde genel olarak üzerinde 5 GHz faaliyet olamaz. Ayrıca yöntem, indüktans yoğunluğunu arttırmak için bir indüktörün spiraller altında Ferromanyetik (FM) çekirdeklerin kullanımını da sağlayabilir. Bu teknik, FM nanopartiküllerinin yüksek geçirgenliği yararlanır. Bununla birlikte, yüksek iletkenlik bu nedenle daha düşük bir Q-faktör indüktör üretilir: Güçlü indüksiyon girdap akımları bir faktördür. Örneğin SU-8 gibi polimerler, çok yüksek olabilir. Örneğin, polimerler ve FM nanopartiküllerin karışım, birden daha yüksek geçirgenlik belli bir değeri vardır. Buna ek olarak, girdaplı akım kayıplarının azaltılması için, bir yüksek bir dirence sahiptir. Dolayısıyla, biz spiral indüktör parçalar arasında bu karışımı kullanabiliriz. Bu şekilde, biz nedeniyle FM malzemenin geçirgenliği yüksek olan, ancak, aynı zamanda, polimerin yüksek direnç için önemli bir kayıp azalmaya endüktans geliştirme değil sadece faydalanabilir

Bu bakış açısı yürütmek için kullanılan yöntemler pratik ve fabrikasyon cihazlar mevcuttur. İlk olarak bir alt-tabaka (silikon veya cam) ve bakır tabakanın üstünde, polimer üzerindeki bakır yatırılır. Daha sonra, Fotolitografi spiral desenler oluşturmak

için kullanılır. Daha sonra, elektriksiz kaplama desen üzerinde bakır yatırmak için kullanılır. Parça açmalarında FM - polimer karışımı ile doldurulur

Anahtar Kelimeler:.Q-factörü, Endüktans yoğunluk, FM-polymer çekirdek, Boy oranı, Geçirgenlik.

To my parents

ACKNOWLEDGEMENT

I sincerely trace my gratitude to Asst. Prof. Dr. Hüseyin SAĞKOL for his honest guidance in my research activities. His generous attitude permitted me to learn a lot both theoretically and practically about my fields of interest.

Further, I would like to acknowledge all other professors such as Assoc. Prof. Dr. Erdal Korkmaz for helping me in my graduate education by providing me solid theoretical backgrounds. I am also thankful to the faculty staffs such as Prof. Dr. Onur Toker for their technical supports.

I am absolutely grateful to my parents for their support in all means and their patience. I would like to also thank my friends and colleagues that embellished my degree with excitations and lots of sportive and recreative activities.

TABLE OF CONTENTS

LIST OF TABLES

TABLE

LIST OF FIGURES

FIGURE

LIST OF SYMBOLS AND ABBREVIATIONS

SYMBOL/ABBREVIATION

A	Cross section area of a metal
B	Magnetic flux density
Bs	Saturation flux density
CMOS	Complementary metal oxide semiconductor
C_{ox}	Oxide capacitance
C_{si}	Silicon capacitance
Cp	Parallel capacitance
E_d	Dissipated energy
FM	Ferromagnetic
GHz	Gigahertz
H	Magnetic field strength
Hc	Coercivity
HAR	High aspect ratio
I	Current
l	Length of a metal segment
l_T	Total length of the spiral
LNA	Low noise amplifier
LO	Local oscillator
Ls	Series inductance
Ms	Saturation magnetization
N	Number of tuns
NF	Noise Figure
nH	Nano-henry (unit of inductance)
Pd	Power dissipated
PDMA	Plating deformation magnetic assembly
Q-factor	Quality factor

Q_c	Quality factor from Y-parameter extraction
Q_{em}	Quality factor from maximum energy calculated
RF	Radio frequency
R_i	Internal radius
Rs	Series resistance
Rsi	Silicon resistance
S	Spacing between metal segments in a spiral inductor
SRF	Self resonant frequency
T_{met}	Metal thickness
T_{sub}	Substrate thickness
V	Applied voltage to the inductor
VCO	Voltage-controlled oscillator
W_m	Maximum magnetic energy
W_{met}	Metal width
W_{pol}	Polymer width
W_{sub}	Substrate width
Φ	Magnetic flux
ρ	Resistivity
σ	Conductivity
μ	Magnetic permeability
μm	Mico-meter
μ_r	Relative permeability
ω	Angular velocity
ω_{Qmax}	Frequency of the maximum quality factor
ω_{SRF}	Self resonant frequency
χ	Magnetic Susceptibility

: : :
: : :

CHAPTER 1

INTRODUCTION TO INTEGRATED SPIRAL INDUCTORS

1.1 APPLICATION OF INDUCTORS IN COMMUNICATION

Inductors are indispensable in the transmission of a signal from one location to another. They are used to temporarily store magnetic energy. The storage of magnetic energy is very crucial in the wireless communication for receiving and transmitting any signal in the electrical form. Figure 1.1 shows the schematic of a simple receiver. This receiver is composed of a Low Noise Amplifier (LNA), a Mixer, a Local Oscillator (LO), a Filter and an antenna.

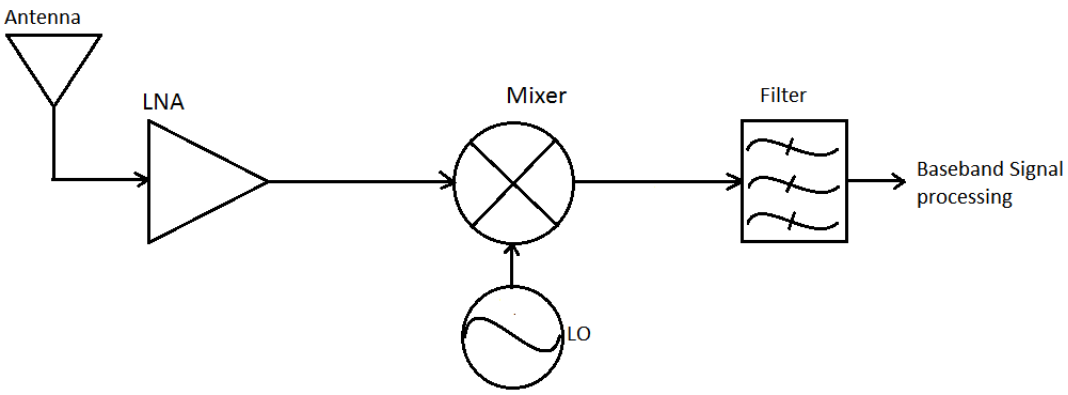

Figure 1.1 A simple RF receiver.

Next, we will discuss the importance of an inductor in each of these parts mentioned above, except for the antenna and the mixer.

1.1.1 LNA

Low noise amplifiers are used to suppress the noise figure (NF) of the succeeding stages. Therefore, one important design factor of an LNA is its gain, which should be as high as possible. Let us consider the simple LNA-Mixer cascade connection shown in Figure 1.2. The total noise figure (NF_{tot}) of the cascade connection can be expressed as follows:

$$NF_{tot} = NF_{LNA} + \frac{NF_{Mix} - 1}{G_{LNA}} \tag{1.1}$$

where NF_{LNA} and NF_{Mix} are the noise figures of the LNA and Mixer, respectively. G_{LNA} is the power gain of the LNA.

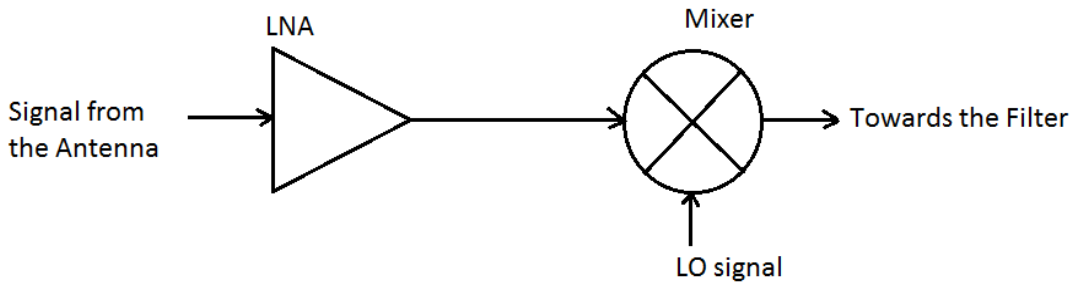

Figure 1.2 Simple cascade connection of LNA and Mixer used in transceivers.

Figure 1.3 shows the circuit representation of an LNA. From Eq. (1.1), we can clearly see that NF_{tot} can be decreased if the gain of the LNA (G_{LNA}) is increased. This power gain of the LNA is proportional to its transconductance (G_m) and its load impedance (Z_L): $G_{LNA} \propto G_m Z_L$

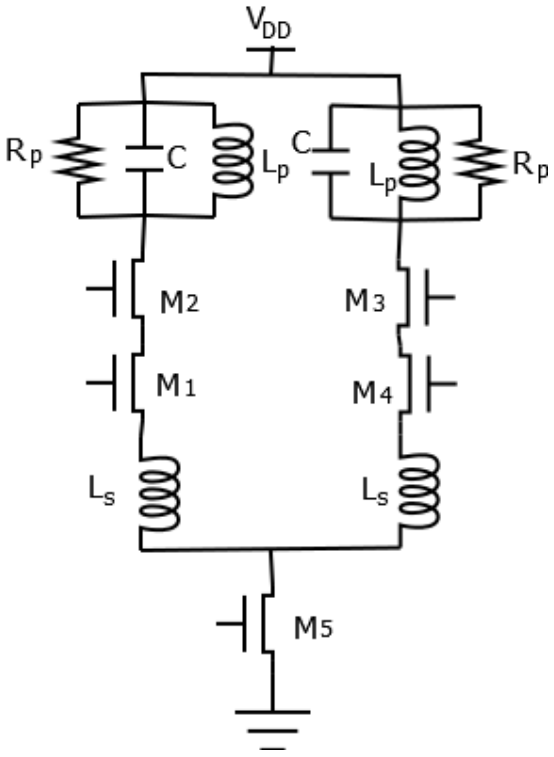

Figure 1.3 Low noise amplifier.

The load impedance (Z_L) is basically an inductor (L) which has a parasitic capacitor (C) in parallel and a parasitic resistor (Rs) in series. Its real part R_{load} is related to its equivalent parallel resistor (R_p) which is proportional to the Q-factor of the inductor as given in Eq. (1.2):

$$R_p = R_s\left(Q^2 + 1\right) \tag{1.2}$$

where Q represents the quality factor of the inductor and is expressed below in equation (1.3):

$$Q = \frac{\omega_0 L_s}{R_s} \tag{1.3}$$

From Eq. (1.2), we can say that the load impedance is proportional to the square of the quality factor of the inductor. Therefore, the LNA needs a high quality factor

inductor in order to have a high gain which is desired for noise suppression of the succeeding stages.

1.1.2 Oscillator

The Voltage-controlled oscillator (VCO) is used as a Local Oscillator (LO). This LO sends a signal at a particular frequency to the mixer which multiplies it with the main signal for up- or down-conversion. The important design factors of a VCO are its phase-noise and power consumption. Figure 1.4 shows a simple VCO configuration.

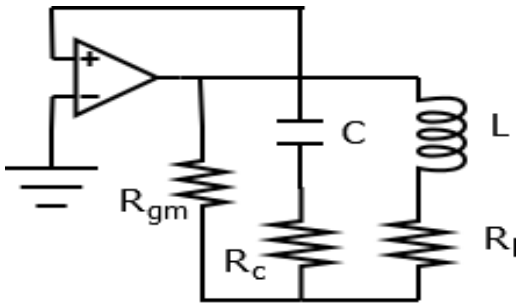

Figure 1.4 A simple Voltage-controlled oscillator.

Next, each of the above design factors will be discussed.

1.1.2.1 Phase-noise

The phase-noise of a VCO should be as low as possible. The phase-noise of the VCO in Figure 1.4 can be expressed as follows:

$$L(\omega) = \frac{2kT\,R_e\,(1+A)}{V^2_{amp}} \times \left(\frac{\omega_0}{\Delta\omega}\right)^2 \tag{1.4}$$

where kT is the thermal energy, A is a constant, ω_0 is the resonant or central frequency of the RLC network, V_{amp} is the amplitude of oscillation, R_e is the effective resistance. This effective resistance can be approximated to the sum of the series resistances of the capacitor and the inductor represented by R_c and R_l, respectively.

$$R_e \approx R_c + R_l \tag{1.5}$$

Nevertheless, the series resistance of the inductor is much larger than that of the capacitor. Therefore, the effective resistance from Eq. (1.5) is reduced to the following:

$$R_e \approx R_l \tag{1.6}$$

One important way of reducing the phase-noise is decreasing the series resistance of the inductor (R_l) which means increasing the Q-factor of the inductor.

1.1.2.2 Power consumption

Another crucial factor that engineers have to consider while designing a VCO is its power consumption. The power consumption of a VCO must be as low as possible in order to reduce its cost. It can be represented by the following equation:

$$G_m = R_e \left(\omega_0 C\right)^2 \approx R_l \left(\omega_0 C\right)^2 \tag{1.7}$$

From Eq. (1.7), the power consumption can be decreased by reducing the series resistance of the inductor.

In sum, a high performance oscillator requires a good quality inductor for the reduction of their noise and power consumption.

1.1.3 Filter

Inductors are actively used in filter designs. LC filters use typically capacitors and inductors connected in series or shunt, as shown in Figure 1.5. A filter must be able to eliminate the unwanted frequency components and keep the desired ones. In order to achieve such requirements, the lumped elements which are inductors and capacitors must be free from any parasitic component. For instance, if an inductor used in a filter has high values of capacitance or resistance, there will be a bandwidth shift from the desired one or power dissipation in the signal as well as noise production. In order to avoid these issues, all the inductors used in a filter must be free from any parasitic element. Note that the capacitors can have relatively high Q-factors, hence they have reduced parasitic effects. Therefore, high Q-factor inductors are strongly required in the

design of filters, especially at microwave frequencies where inductors are prone to parasitics.

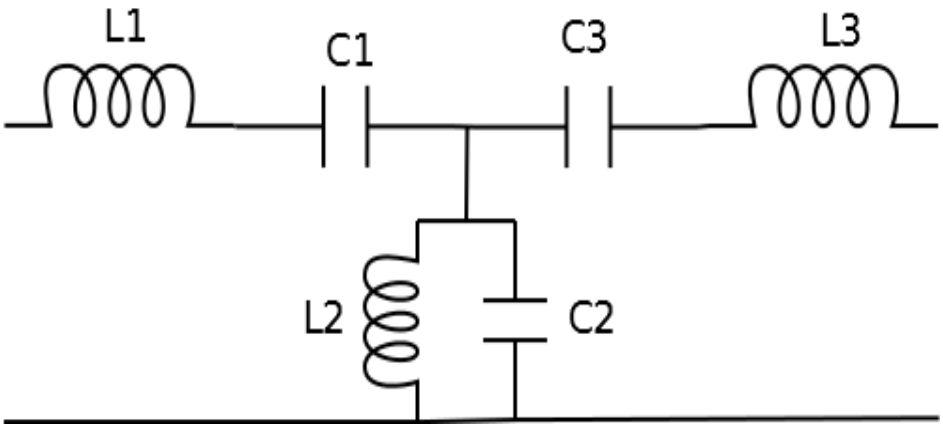

Figure 1.5 RF Bandpass filter.

1.2 LITERATURE SURVEY

The idea of integrating inductors dates several decades ago. Spiral inductors are simpler and easier to fabricate and optimize when compared to their solenoidal counterparts. The very first spiral inductors used in general GaAs substrates and were very large in size with only few nano Henrys inductance. In 1984, a group of scientists have modeled a MMIC spiral inductor with high accuracy [1]. It uses a GaAs substrate and has a relatively large size, even though it has a high cutoff frequency. Further, the first computer aided design of a square shape spiral inductor was implemented by K. Araki, H. Ueda and M. Takahashi [2] in 1985. Beside using a GaAs substrate, this inductor was showing relatively high losses for a 0.2 mm size. Due to their substrate nature and large footprint, the previous inductors could not be integrated in our daily ICs which use silicon substrates in general. Therefore, Attentions have been put into employing silicon substrates for designing spiral inductors. However, the lossy nature of Silicon substrates caused many challenging issues. In 1996, a publication by Yue and others [3] demonstrated the effects of parameters such as substrate resistivity, oxide thickness and metal thickness on the quality factor of the inductor. This paper outlined the Q-factor reduction of low resistivity substrates and thin-layer oxide inductors. Further publications include [4] where the effect of the inductor's physical geometry modifications has been analyzed.

Many techniques have been employed by researchers for the sake of producing high quality factor spiral inductors using silicon substrate. In 1998, Yue and Wong produced spiral inductors using different ground shields [5]. Although a Q-factor improvement was observed, the inductance decreases exponentially at frequencies above 2 GHz and the inductor's footprint is large. Xiangming Xu and others have implemented a multiple layer stacked spiral inductor (in 2012) [6]. The results have shown that even thought the quality factor improves with the staking layer, the self-resonant frequency is too low with three or more stacking layers. In 2013, J. Zhan and others have used two different FM nanoparticle cores in multilayer spiral inductors [7]. The results show a huge improvement in the inductance density. However, the process is very expensive and the Q-factor is poor beyond 2.5 GHz. Despite myriads of optimizations throughout couple decades ago, the implemented

inductors are not still satisfactory in general to overcome the integration issues for high frequency applications. Therefore, an initiative consisting of mixing insulating polymer and FM nanoparticles is a novel idea that can considerably augment the Q-factor of a spiral inductor. This mixture results in a semi-magnetic core that has fairly good permeability and high resistivity, hence the inductance density and self resonant frequency can be high, as expected.

In this paper, we will first present a descriptive study of the spiral inductors in Chapter 2 which is followed by Magnetic induction mechanism along with well-known inductor models in chapter 3. Next, we will discuss the quality factors and optimization methods presented in previous works in Chapter 4. Further, the design and fabrication of our Spiral inductor will be given in Chapter 5. Lastly, Chapter 6 will contain the Results of our measurements and a Conclusion.

CHAPTER 2

A DESCRIPTIVE STUDY OF ON-CHIP SPIRAL INDUCTORS

A detailed study to understand the physical composition of a silicon substrate spiral inductor and the loss mechanism occurring during its operation will be given in this chapter. Further, the parasitic and proximity effects on silicon substrate inductors will be discussed.

2.1 DESCRIPTION OF ON-CHIP SPIRAL INDUCTORS

The simple pi-model on-chip spiral inductor shown in Figure 2.1 (a) is the most well-known. It is composed of a spiral metal track on top, an oxide layer beneath the metal track and a silicon substrate at the bottom (Figure 2.1). Often, there are some epitaxial layers between the oxide layer and the silicon substrate for performance improvement purpose.

The metal can be copper or aluminum, although the former is the most common due to its high conductivity. It can be in the rectangular (or square), polygonal or circular shape as seen in Figure 2.1 (b). Although the circular shape spiral inductor is the most area efficient, its fabrication requires sophisticated tools which makes it less practical compared to its polygonal and rectangular counterparts. Therefore, the rectangular shape spiral inductor is the easiest and most practical. The oxide layer is usually a thin layer and consists of silicon dioxide (SiO_2) for the most cases. The silicon substrate is relatively thick and is the most loss-prone layer in the inductor configuration since they naturally have low resistivity. On the other hand, a high resistivity silicon substrate can be used to decrease the loss.

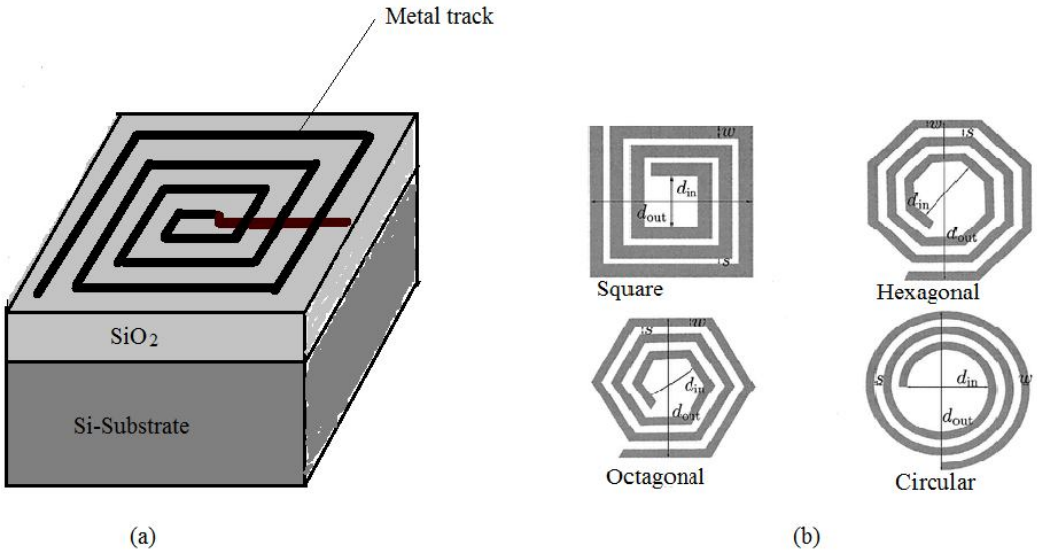

Figure 2.1 (a) Silicon substrate spiral inductor using square shape metal, (b) Different shape representations of the metal in spiral inductors.

Next, We will analyze the losses that accompany the inductance of the silicon substrate spiral inductor.

2.2 LOSS MECHANISM OF ON-CHIP SPIRAL INDUCTORS

2.2.1 General Overview

On-chip planar inductors face significant losses that reduce their inductance values and self resonant frequencies (SRF) during their operation. An applied time varying voltage creates a current that induces three electric fields and one magnetic field as se en in Figure 2.2.

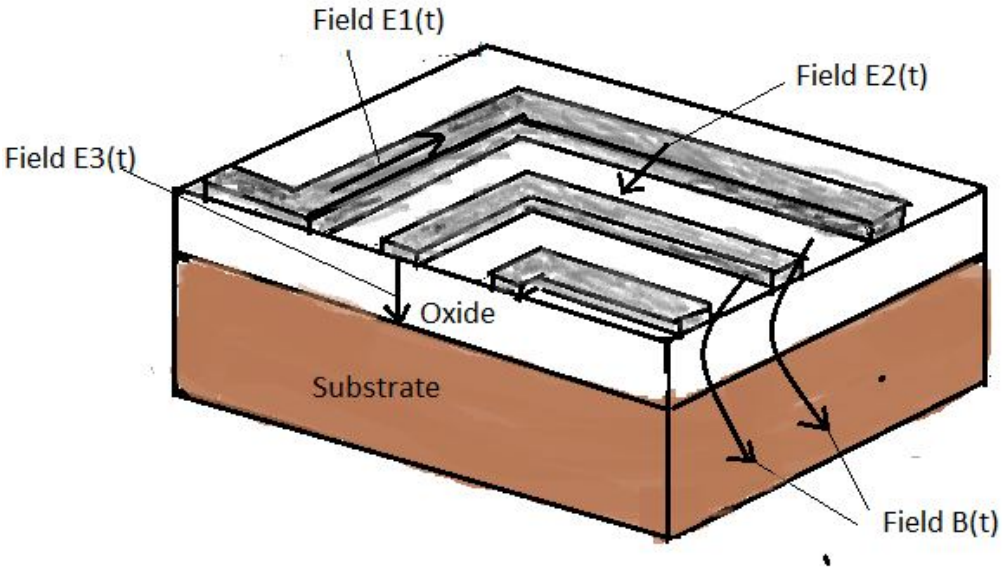

Figure 2.2 Fields generated in on-chip inductors after an applied time varying current.

- Electric field E_1 (t) along the spiral: It is the result of potential difference between the two ends of the spiral. It results in some ohmic losses along the spiral due to the metal resistivity. This resistivity is constant at low frequencies. However, it becomes significant and frequency dependant at higher frequencies because of the *skin effect*. The amount of ohmic loss is determined by the metal properties. High conductance metals produce less loss and high magnetic flux.

- Electric field E_2 (t) between the strips: It is caused by the potential difference between the adjacent strips. It results in electrical coupling between the strips that has a parasitic effect on the inductance value and decreases the self resonant frequency (SRF). Nevertheless, the effect of this capacitive coupling becomes significant only at very high frequencies, though it is taken into account in most designs.

- Electric field E_3 (t) between the metal and the substrate: This field is obtained due to the displacement charges from the high potential metal to the zero potential substrate. Consequently, it produces a displacement current hence some ohmic loss and also a capacitive coupling between the metal and the substrate. It causes the most important electrical coupling effect in the operation of on-chip inductors.

- Magnetic field B(t): The time varying current applied to the inductor creates a magnetic field B(t) due to the metal's magnetic properties (Ampere's law). This time varying magnetic field penetrates into the silicon substrate and induces some eddy current (Lenz' law) because of its low resistivity. Since the flow of the current always face some resistance, we will have some ohmic losses due to the substrate resistivity. On the other hand, the induced magnetic field B (t) creates self and mutual inductances. Self inductance and positive mutual inductance are indeed desired from the inductor.

2.2.2 Metal Losses

The losses produced in the metal are determined by three important factors: the ***DC series resistance***, ***the skin effect*** and the ***current crowding effect***. These factors are directly or indirectly related to the frequency of operation

2.2.2.1 DC series resistance

Denoted by R_{dc}, it is important at low frequencies and insignificant at higher frequencies. It is proportional to the resistivity (ρ) of the metal and the length of the coil, and inversely proportional to the width w and the thickness (t) of the coil. The resistivity of the metal is constant at low frequencies, hence the DC series resistance is frequency independent as given in the Eq. (2.1).

$$R_{dc} = \rho \frac{l}{w \cdot t} \tag{2.1}$$

where l, w and t are the length, the width and the thickness of the conductor, respectively. They are given in meter.

2.2.2.2 Skin effect

The skin effect is a very important factor that occurs at high frequencies. It is basically the fact that the current displacement along the spiral which is initially in inner surface is deviated toward the outer surface due to an internal magnetic force, as shown in Figure 2.3. This magnetic force is emanated from the time varying magnetic field created by the applied current or say voltage, which penetrates in the conductor. The skin effect increases the effective resistance due to the decrease in the effective cross section area of the conductor. It is determined by the skin depth (δ) which is the equivalent thickness of the conductor at a specific frequency. It is related (inversely) to the magnetic permeability (μ), the conductivity (σ) and the frequency (ω). We can write the following equation for the skin depth (in meter).

$$\delta = \sqrt{\frac{2}{\mu \cdot \delta \cdot \rho}} \tag{2.2}$$

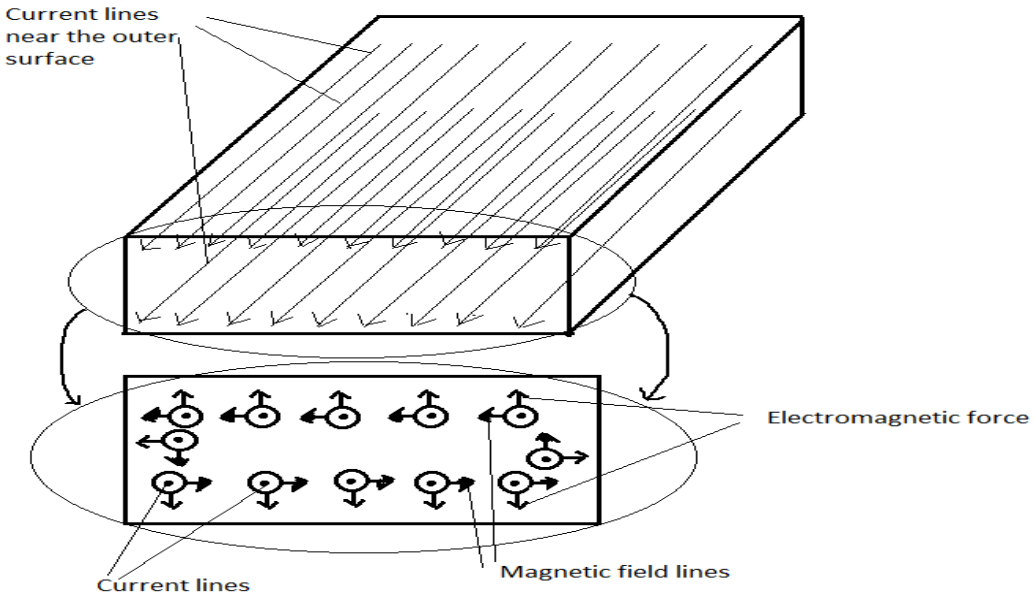

Figure 2.3 Skin effect on a metal.

2.2.2.3 Current crowding effect

The current crowding effect or proximity effect occurs when the magnetic field of a strip induces current in the neighboring strip. This induced eddy current forms loops along the strip as shown in the Figure 2.4. It adds to the excitation current in the inner edge and subtracts to it in the outer edge. This non-uniformity of the current density augments the effective resistance of the metal.

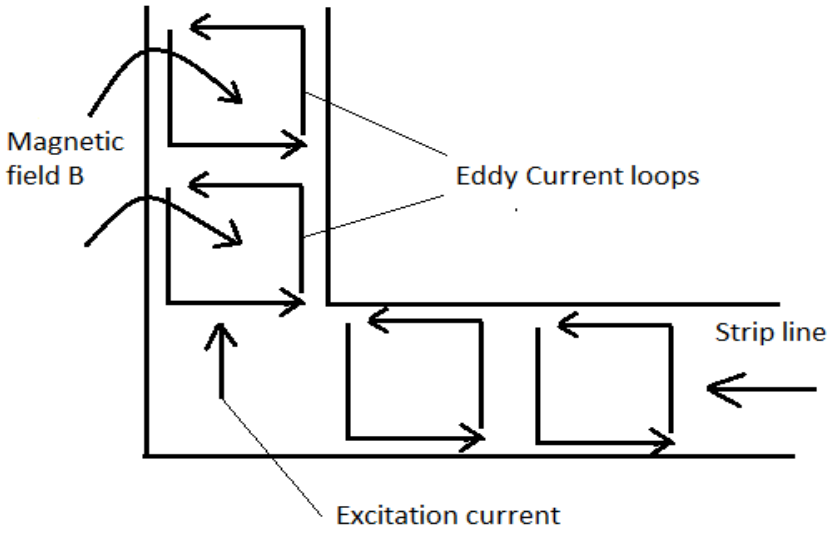

Figure 2.4 Eddy current in a metal.

The skin and current crowding (or proximity) effects change the effective resistivity or effective thickness t_{eff}. Therefore, Eq. (2.1) can be reformulated as follows:

$$R_s = \rho \frac{l}{w \cdot t_{eff}} \tag{2.3}$$

where Rs is the series resistance expressed in Ohm (Ω), t_{eff} is the effective thickness (in meter) of the metal which is expressed below:

$$t_{eff} = \delta \cdot \left(1 - e^{-t/\delta}\right) \tag{2.4}$$

As we see, the effective thickness decays exponentially and is a function of the skin depth δ and the physical thickness t.

2.2.3 Substrate Losses

The On-chip inductors use in general low resistivity silicon substrates. Therefore, they are very prone to substrate losses which decrease the inductor's quality factor. These losses results from two effects: The capacitive coupling effect and the inductive coupling effect.

- The capacitive coupling effect occurs because of the potential difference between the metal and the substrate, as mentioned before. This coupling creates displacement current in the substrate, hence some ohmic losses which will be represented as a resistance in the inductor circuit model representation. These losses can be considerably decreased when high resistive substrates are used.

- The inductive coupling effect occurs when the magnetic field created from the metal penetrates in the substrate and induces eddy current due to Lenz' law. This eddy current is very important, especially when the substrate is less resistive and causes significant losses in the substrate. Figure 2.5 shows the capacitive and inductive effects on the substrate.

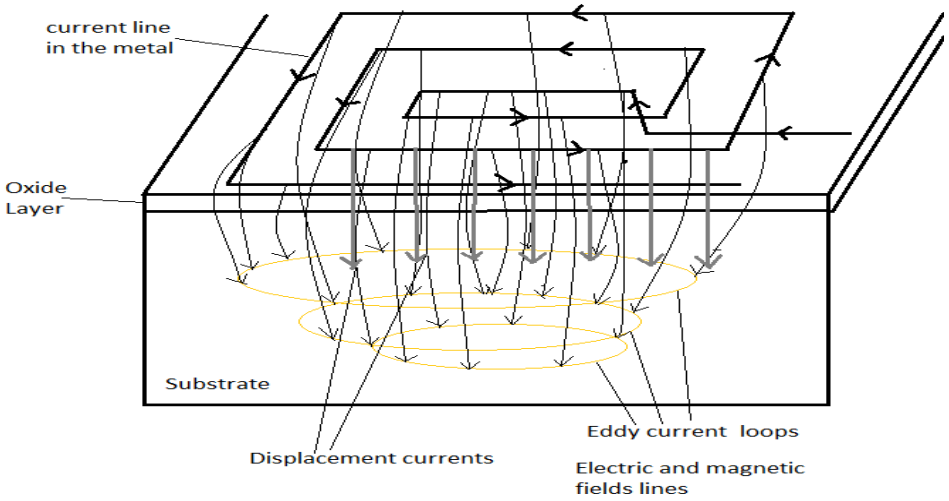

Figure 2.5 Capacitive and inductive coupling effects on a silicon substrate.

2.3 PARASITIC EFFECTS

In addition to the loss mechanism, the parasitic mechanism is another phenomena that reduce the inductor's quality factor as well as its self resonant frequency. It happens simultaneously with the loss mechanism, however, it accounts its own effect separately from that of its loss mechanism counterpart. There are basically two types of parasitic effects: ***electrically induced parasitic effect*** and ***magnetically induced parasitic effect***.

2.3.1 Electrically induced parasitic effect

It is due to the electrical coupling between the coils of the metal and between the metal and the substrate as shown in Figure 2.6. They form a sort of capacitances that consumes up the energy stored in the inductor. Hence the inductance decreases while the capacitance increases. At frequencies higher than the self resonant frequency, the inductor behaves like a capacitor and becomes useless.

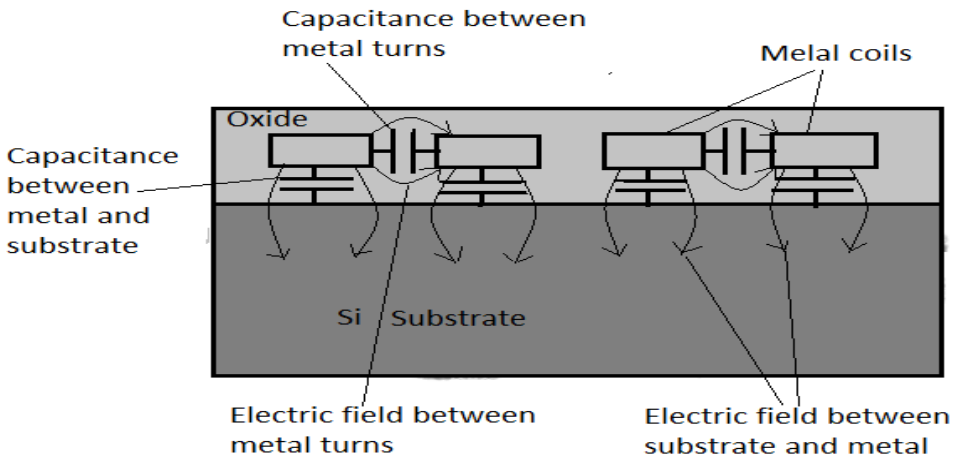

Figure 2.6 Parasitic capacitances of a single-layer spiral inductor.

The above figure typically represents the parasitic capacitance between the metal tracks and between the metal and the substrate for a single-layer integrated spiral inductor. However, the inductor can have several metal layers for some applications. In

that case, the capacitance between metal layers will also account for the parasitic capacitances which will therefore increase. We will analyze this effect under the stacked inductors in later chapters. Another parasitic capacitance comes from the capacitive nature of the substrate. It is due to the local potential differences in the substrate after electric field penetration. However, it is not very crucial. The most important capacitance lies between the metal and the substrate.

2.3.2 Magnetically induced parasitic effect

The magnetic field created from the metal penetrates in the substrate and induces eddy current loops (see Figure 2.7). The induced eddy current also creates some magnetic field that will oppose to the primary field, hence it forms a negative mutual inductor that reduces the total inductance. The negative mutual inductance can be formed between the metal tracks also as shown in Figure 2.7.

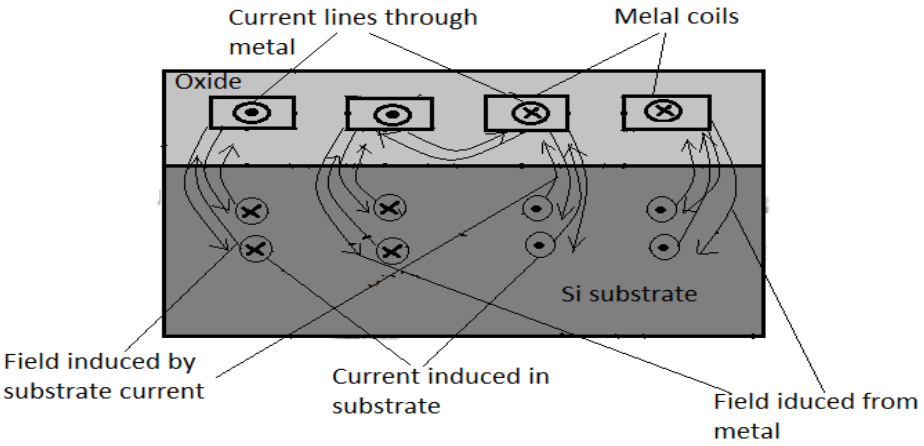

Figure 2.7 Magnetic coupling between metal tracks and the substrate.

The eddy current formation in the substrate is one of the most important phenomena that weaken the quality factor of a spiral inductor. Its effect decreases with the resistivity of the substrate. In another word, the more the substrate is conductive, the

more it is prone to eddy current formation. Therefore, high resistivity substrates are preferred to overcome this issue.

CHAPTER 3

MAGNETIC INDUCTION THEORY AND ON-CHIP INDUCTOR MODELS

In this chapter, the common method of calculating the inductance of a spiral inductor is presented. The effect of inductor geometry change is later analyzed. Further, the schematic representations of different inductor models are given.

3.1 INDUCTANCE CALCULATION

3.1.1 Self Inductance

When we apply a time varying voltage to the two ends of a conductor line, a time varying current (I) flows through the conductor and creates a magnetic field (**B)** as shown in Figure 3.1. Eq. (3.1) gives the magnetic field vector (**B)** at any distance (r).

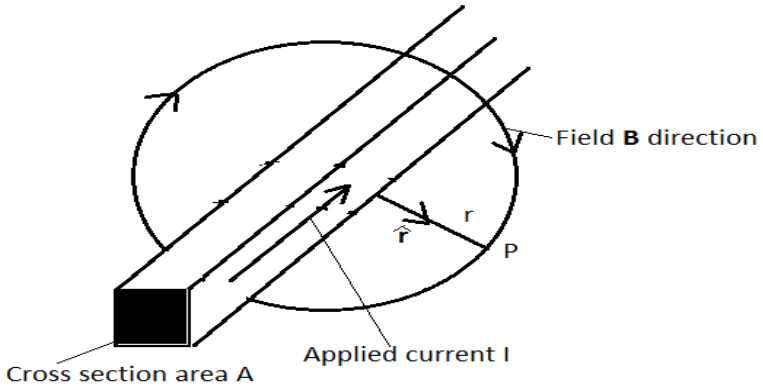

Figure 3.1 Magnetic induction of a wire.

$$\mathbf{B} = \frac{\mu I}{4\pi}\int_{l1}^{l2}\frac{d\mathbf{l}\times\hat{\mathbf{r}}}{r^2} \tag{3.1}$$

where μ is the magnetic permeability of the medium; r is any distance from the conductor; **l** is a unit vector that follows the current flow through the conductor; I is the current flowing through the conductor. The magnetic field **B** is given in T (tesla).

The magnetic field **B** creates a magnetic flux which is proportional to the cross section area A of the conductor, as given in Eq. (3.2). The Unit of magnetic flux is Webber (Wb).

$$\Phi = \mathbf{B}\cdot\mathbf{A} \tag{3.2}$$

where Φ and **A** are the magnetic flux and cross section area of the conductor, respectively. The magnetic flux is non-zero if the field is not parallel to the surface of the conductor, as shown in Figure 3.2.

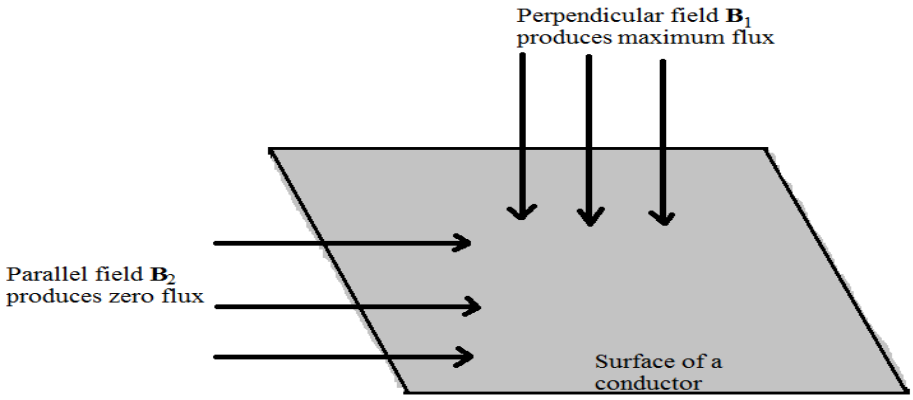

Figure 3.2 Magnetic flux production.

Furthermore, the magnetic flux is related to the current by a proportionality constant called inductance. In another word, the inductance L is defined as the ratio of total magnetic flux to the current.

$$L = \frac{\Sigma\Phi}{I} \tag{3.3}$$

where L is expressed in Henry (H).

To calculate the self-inductance of complex structures such as spiral inductors, Eq. (3.3) is used as point of depart. Nevertheless, this equation can be modified and reduced to an expression containing solely the dimensions of the metal line. Thus, for a metal segment of width w, length l, and thickness t, the self inductance can be given by Eq. 3.4.

$$L_{self} = 2l\left[\ln\left(\frac{2l}{w+t}\right) + 0.5 + \frac{w+t}{3l}\right] \tag{3.4}$$

The self inductance L_{self} is expressed in nano-Henry (nH).

The approximate formula for calculating the total self inductance of a square-shape spiral inductor is given in Eq. (3.5):

$$\sum L_{self} = \frac{\mu_0}{4\pi} l\left[\ln\left(\frac{l_T}{n(w+l)}\right) - 0.2\right] \tag{3.5}$$

where l is the average length of all segments; μ_0 the free space magnetic permeability; w the width of the segments; l_T the total length of the spiral.

3.1.2 Mutual inductance

The concept of mutual inductance comes from the influence of the magnetic field of a coil on his neighboring coil. The mutual inductance M_{12} of coil 1 and coil 2 is the ratio of magnetic flux Φ_{12} (or Φ_{21}) of coil 1 on coil 2 to the current I_1 flowing through coil1 as given in Eq. (3.6)

$$M_{12} = \frac{d\Phi_{12}}{I_1} \tag{3.6}$$

M_{12} is given in H.

Eq. 3.6 is the general formula of mutual inductance. If the coils are parallel, Eq. (3.6) leads to Eq. (3.7) which contains only the physical parameters of the coils, as given below:

$$M_{12} = 2lQ \tag{3.7}$$

where l is the length of the coil and Q is a coefficient that depends on the coil geometry. Q can be expressed in Eq. (3.8):

$$Q = \ln\left\{\frac{1}{GMD} + \left[1 + \left(\frac{l}{GMD}\right)^2\right]^{1/2}\right\} - \left[1 + \left(\frac{GMD}{l}\right)^2\right] + \frac{GMD}{l} \tag{3.8}$$

where GMD is denoted as geometric average of distance between the areas of the two conductors.

The coefficient Q is related to the coil length l and the geometric average of distance GMD between the areas of conductors. The GMD is the average distance between the surfaces of two conductors. It can be obtained by dividing these surfaces into several unit areas as shown in Figure 3.2.

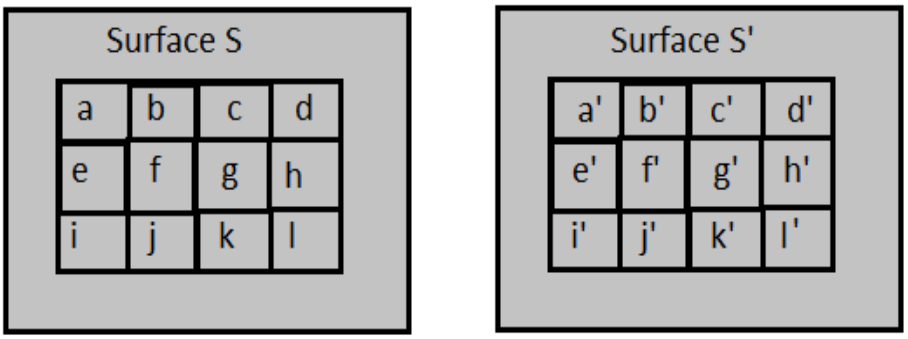

Figure 3.3 Computation of GMD by surface division.

Further, Eq. (3.9) is applied to find the value of GMD.

$$GMD = \sqrt[m \cdot n]{D_{aa'} \cdot D_{ab'} \cdots D_{ba'} D_{bb'} \cdots} \tag{3.9}$$

Where m and n are the number of unit surfaces on surface S and S′ respectively; Daa′, Dab′,… are the distances between unit surfaces a, b,… and unit surfaces a′, b′…, respectively.

If the conductors have a rectangular shape, Eq. (3.9) is modified to Eq. (3.10) as follows:

$$\ln(GMD) = \ln(d) - \frac{W^2}{12d^2} - \frac{W^4}{60d^4} - \frac{W^6}{168d^6} - \frac{W^8}{360d^8} - \dots \tag{3.10}$$

where W is the center to center width and d the center to center distance.

When we increase the center to center spacing, the mutual inductance decreases as shown in Figure 3.4. Similarly, the decrease in the width of the conductors decreases the mutual inductance.

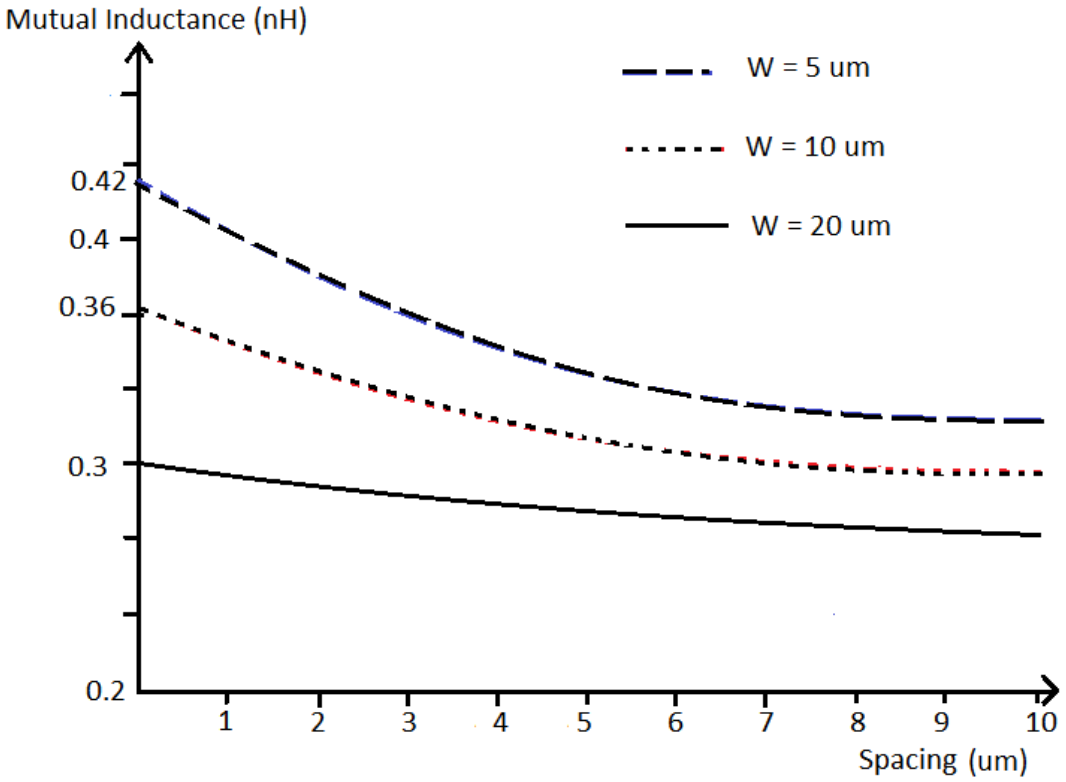

Figure 3.4 Sketch of mutual inductance versus the spacing for different center to center widths for two parallel rectangular conductors with 1 μm thickness.

The mutual inductance can be positive or negative depending on the directions of the magnetic fields generated by the two lines. In another word, the mutual inductance is positive when the current flow direction is same in both lines and negative if the two lines have opposite current directions, as shown in Figure 3.5.

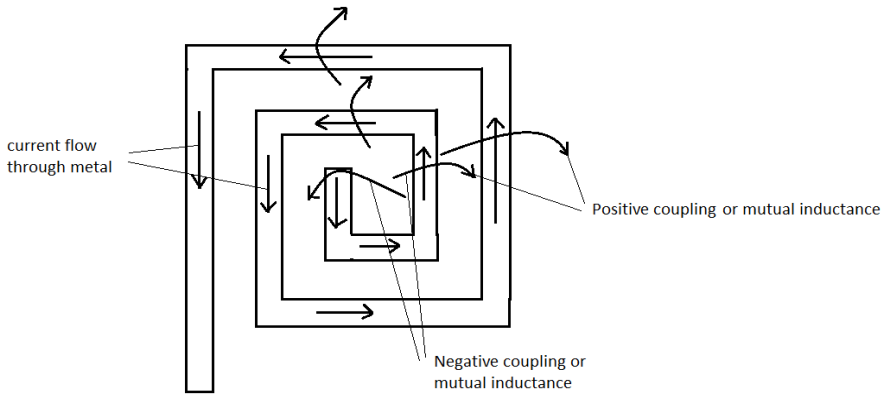

Figure 3.5 Positive and negative mutual inductances of a square-shape spiral inductor.

In general, the mutual inductance depends on the spacing between the two conductors, their crossing angle and their lengths. There is no mutual inductance between orthogonal lines because their magnetic fields do not affect each other.

The total positive and negative mutual inductances of a square-shape spiral inductor are expressed in Eq. (3.11) and (3.12), respectively.

$$\sum M_{+} = \frac{\mu_0}{4\pi} l_T (n-1)\left[\ln\left(\frac{l_T}{4nd} + \sqrt{1+\left(\frac{l_T}{4nd}\right)^2} \right) - \sqrt{1+\left(\frac{4nd}{l_T}\right)^2} + \frac{4nd}{l_T} \right] \tag{3.11}$$

$$\sum M_{-} = \frac{\mu_0}{4\pi} l_T \frac{n}{214} \tag{3.12}$$

Where lT is the total length of the spiral; n is the number of turns; d is the average distance of all segments. The above equations are valid for only square shape-spiral inductors.

3.1.3 Total inductance

The total inductance is calculated by summing the self and positive mutual inductances and subtracting the negative mutual inductance as given in Eq. (3.13).

$$L_{total} = \sum L_{self} + \sum M_{+} - \sum M_{-} \tag{3.13}$$

where L_{total} is the total inductance; M_{+} and M_{-} are the positive and negative mutual inductances, respectively.

3.2 EFFECTS OF THE SPIRAL INDUCTOR PARAMETERS'CHANGE

The primary way of changing the quality factor and the inductance value of an integrated inductor is to play with its geometrical parameters such as width, length, spacing...Some changes can be theoretically understood, however some others are only understood through experiment. In this section, we will analyze the effects of changing the basic geometrical parameters of integrated spiral inductors.

3.2.1 Side number

Keeping the external radius fixed, if we increase the number of sides of a spiral inductor, its perimeter will increase. So the total length of the spiral will increase. Increase in total length means an increase in inductance as observed in Eq. (3.4). However, the resistance also will increase, although it is not crucial compared to the increase in inductance. Although the skin effects were not accounted, the resultant quality factor of the inductor increases when we increase the number of sides.

To be more realistic, let's compare a square and circular shapes, spiral inductor as shown in Figure 3.6.

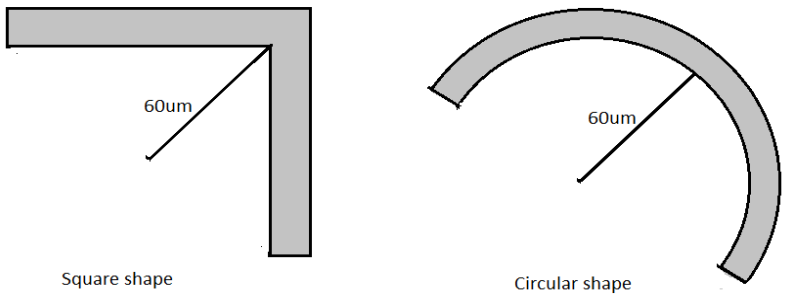

Figure 3.6 Comparison of a Square and circular shape spiral inductors.

The half-section inductors in Figure 3.5 have same diameters and operate at 1.8 GHz. Table 3.1 shows the values of different measured parameters such as inductance, resistance and Q-factor.

Table 3.1 comparison of square-shape and circular-shape inductors.

	Square geometry	Circular geometry
Inductance (nH)	0.05	0.06
Resistance (Ω)	0.0424	0.0471
Quality factor	13.3	14.4

From Table 3.1, we can conclude that the Q-factor produced by the circular-shape inductor is greater than that produced by the square-shape inductor.

Further, several inductors with different side numbers are simulated using ASITIC tools. Figure 3.7 shows the approximate plot of the quality factor versus the number of sides.

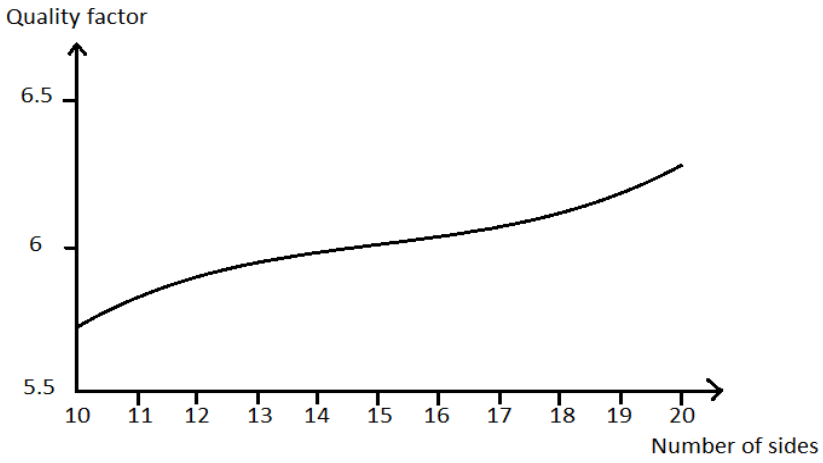

Figure 3.7 Graph of side number influence on quality factor of spiral inductor.

Graph 3.7 tells us that the quality factor of an on-chip spiral inductor increases with the number of sides.

3.2.2 Spacing between tracks

Just like the side number, the analysis of the spacing between tracks can be understood without any empirical data. When we decrease the spacing between the

tracks without changing the length of the metal and keeping the internal radius constant, the positive mutual inductance (which is dominant over its negative counterpart in metal) increases while the resistance is kept constant. Therefore, the quality factor improves. However, increasing the spacing between the metal tracks results in a decrease in the inductor's quality factor. For instance, small spacing is required between the tracks. Figure 3.8 shows an approximate trace of an inductor's quality factor versus frequency for different spacing between the metal tracks.

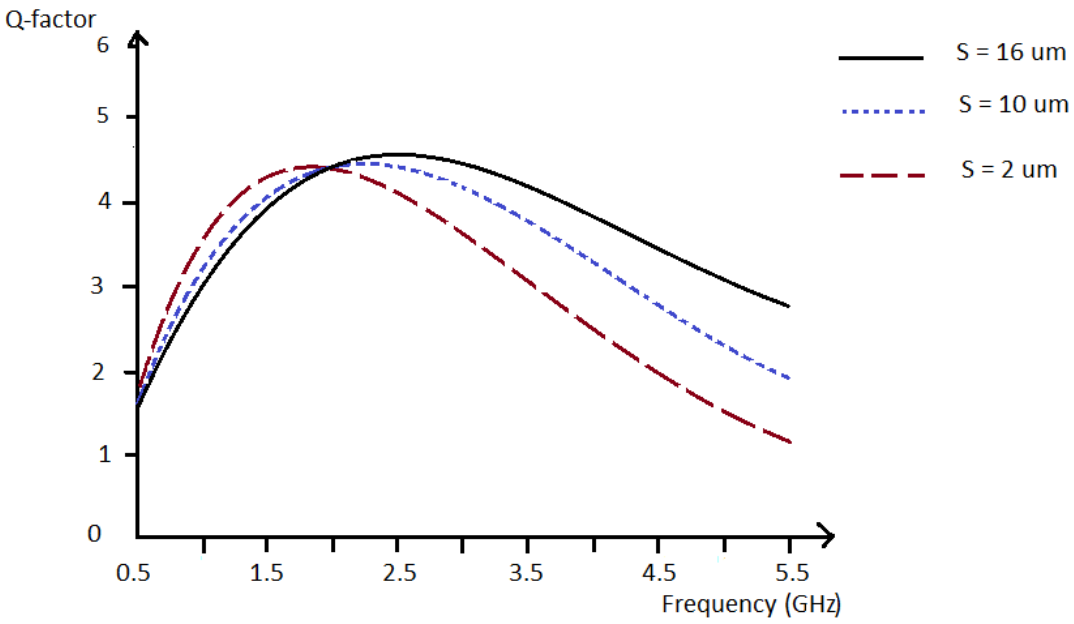

Figure 3.8 Plot of spacing (S) influence on quality factor of a spiral inductor.

Although decreasing spacing increases Q-factor of the inductor, the frequency of operation has to be considered. As shown on Figure 3.8, higher spacing is better for some frequencies (e.g.: From 2 GHz to 5.5 GHz on the graph). The small spacing is not preferred at higher frequencies because the capacitance between the tracks also increases, which is parasitic to the inductance value resulting in a poor Q-factor.

3.2.3 Number of turns

The influence of the number of turns is not so simple to analyze. Many factors have to be accounted precisely in order to determine the effect of the turns. Keeping other parameters constant, an increase in the number of turns leads to the following:

- An increase in the inductance due to increase in the magnetic field;

- An increase in the metal resistance. More turns means increase in length, so in the resistance;

- An increase in the parasitic capacitance between the metal tracks. This is due to the increase in the effective areas of metal track among each other;

- An increase in the coupling capacitance between the metal and the substrate due to augmentation of space occupied by the metal turns. So the maximum Q-factor value will be shifted to lower values;

- An increase in the eddy current induced in the substrate because of an increase in the magnetic field. So the negative mutual inductance also increases.

Taking into account all these effects, one cannot simply determine theoretically whether an increase in the number of turns results in an increase or decrease in the quality factor. Therefore, an empirical analysis is necessary to determine the effect of turns more realistically. Figure 3.9 shows a reproduced ASITIC simulation result of the quality factor of a spiral inductor for different number of turns.

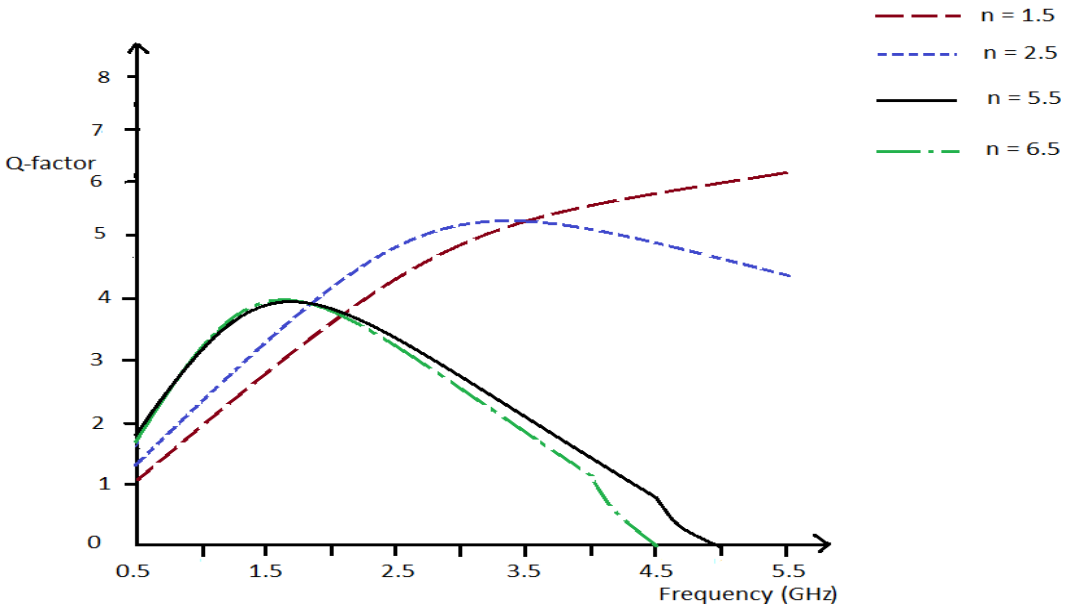

Figure 3.9 Graph of turn number influence on the quality factor of a silicon substrate spiral inductor.

As we observe from the graph, if the number of turns is high, the maximum quality factor is shifted left to the lower frequencies. Therefore, the higher turn number is preferred at lower frequencies. In contrast to high turn-number inductors, the Q-factor is higher for inductors with lower turn numbers at high frequencies. Nevertheless, the inductance value is also lower.

3.2.4 External radius

The external radius is another parameter that needs empirical analysis in order to see its exact effects. However, it has to be selected so that the internal radius is not too small. If the internal radius is small, a strong negative magnetic coupling is created in that area, and the total inductance will be reduced. In addition, there will be a high capacitance value between metal tracks which will reduce the self resonant frequency.

3.2.5 Width

One way to decrease the DC resistance of the conductor is to increase its width. In contrast, increasing the width to a certain value encounters several issues. As proved in Eq. (3.5), the inductance is inversely related to the width, therefore it becomes smaller

when the width is increased. Increasing the width results in an increase in the area occupied by the metal and hence the coupling capacitance to the substrate increases. Large metal width is impractical at high frequencies due to the skin effect. Therefore, the knowledge of the metal skin depth is important before increasing the metal width. However, a deep theoretical study is needed to determine the skin effect on the metal width.

Let us analyze the skin effect on a rectangular aluminum coil, although the copper coil is becoming common due to its lower DC resistivity. By taking the fixed value of skin depth at a specific frequency (e.g.: 1 GHz) and calculating the skin effect on the aluminum, it has been observed that the skin effect is only serious after a higher frequency (e.g. 8 GHz). However, experiments show that the skin effect influences the metal at much lower frequencies. Therefore, there must be an additional effect affecting the rectangular metal which is called ***corner effect***. The non-symmetric current distribution at the corners of a rectangular conductor leads to an increase in the metal effective resistance at high frequencies.

In order to analyze the skin and corner effects of the metal, a simulation that relates the resistive effects to frequencies is presented for different metal widths. The results of simulators are depicted: HP momentum and Media sonnetlite. Figure 3.10 shows the simulation results.

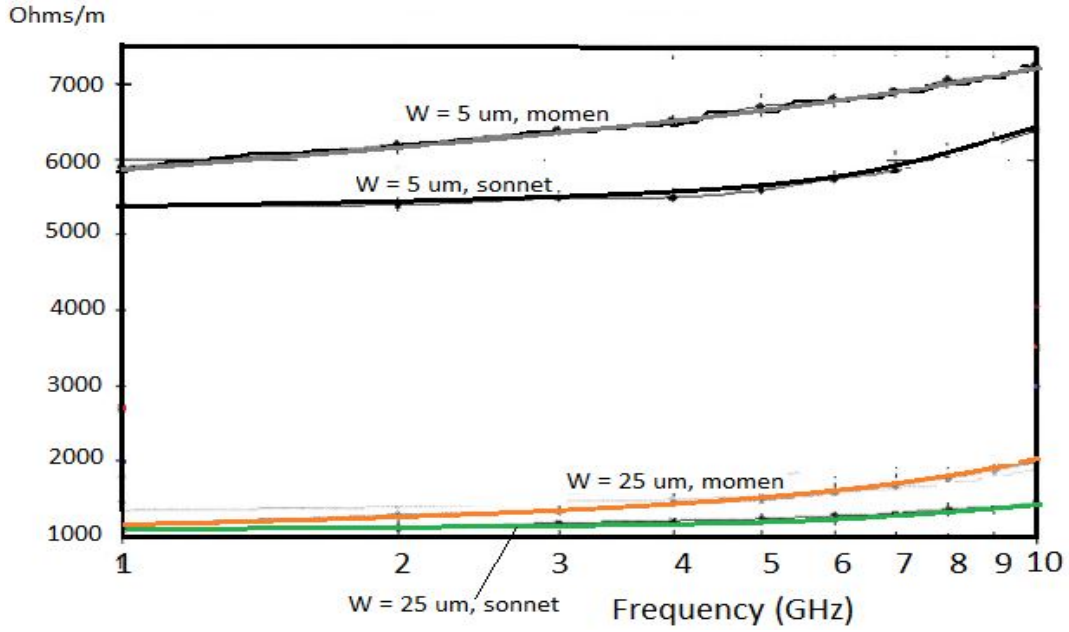

Figure 3.10 Plot of resistance over frequency for different metal widths.

As we observe from the graph, the corner effect is more significant when the metal width is smaller (less than 10 um). This is due to high DC resistance in small width conductors. On the other hand, when the width is too high (more than 20 um), the inductance per unit length decreases. Therefore, it is recommended to choose the inductor's width between 10 um and 20 um.

At lower frequencies (1 GHz to 5 GHz), the corner effect acts as a parasitic. Therefore the inductor' s quality factor is poor. Nevertheless, when the frequency increases, the skin effect is also introduced to increase the resistance and make the quality factor even poorer.

3.2.6 Parallel metal layers

When parameters like metal length, width and resistivity are fixed, one convenient way to decrease the metal resistance is to increase its thickness. This can be achieved by building several metal layers in parallel. The effective thickness decreases, so does the DC resistance. On the other hand, the coupling capacitance to the substrate also increases, decreasing the self resonant frequency (SRF). However, the resistance

reduction is so significant that the coupling effect can be ignored. It is preferable to make two to three parallel layers.

There are many ways of building the layers in parallel. Figure 3.11 shows different techniques of paralleling the metal layers.

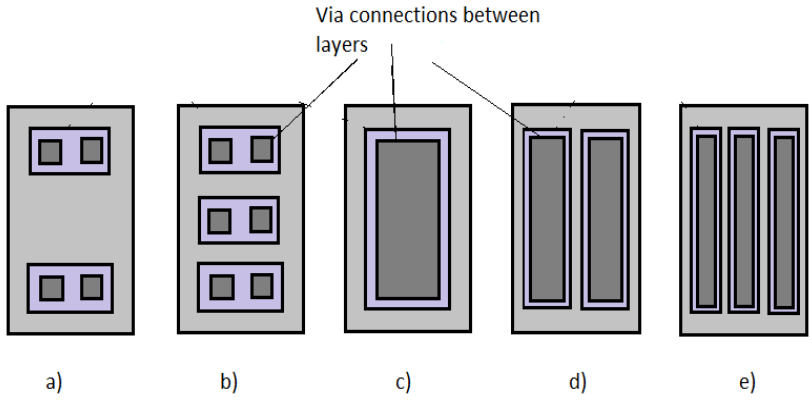

Figure 3.11 Different methods of paralleling metal tracks.

As see from the figure, the vias can be built horizontally (a and b) or longitudinally (c, d, and e) between the layers of connections.

As an example, we shall consider the two-layer inductor in Figure 3.12 where the metal tracks are connected by a longitudinal via connection. The tracks width and length are 12 µm and 80 µm respectively. The via length is varied between 10 µm and 30 µm with an increment of 10 µm. AC simulation is used and the impedance of the inductor is measured.

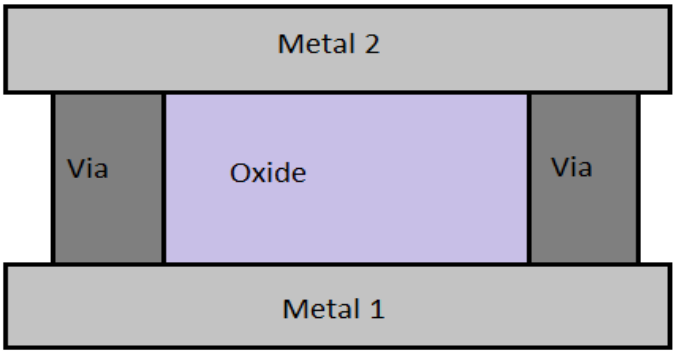

Figure 3.12 Metal layers connected by longitudinal vias.

Further, the inductance and resistance changes are recorded in Table 3.2. Note that this result is valid for all different widths of connections.

Table 3.2 Change in Inductance (ΔL) and Resistance (ΔR) as a result of via connection between the two layers of a spiral.

ΔArea (%)	ΔL (%)	ΔR (%)
100	15	35
200	28	55
300	39	62

3.3 INDUCTOR MODELS

There are several models of the spiral inductors. However the most common ones are the π-model, the transformer model and the wideband π-model. Indeed, the π-model is the most used. We will briefly present each model.

3.3.1 Pi-Model

As we have stated before, the π-model spiral inductors are very flexible and easy to design. Their parameters can be easily changed to an optimum. However, they operate in a very narrow frequency range. Therefore, this model is best for a single frequency operation. Figure 3.13 shows the circuit representation of the Pi-model spiral inductor with silicon substrate.

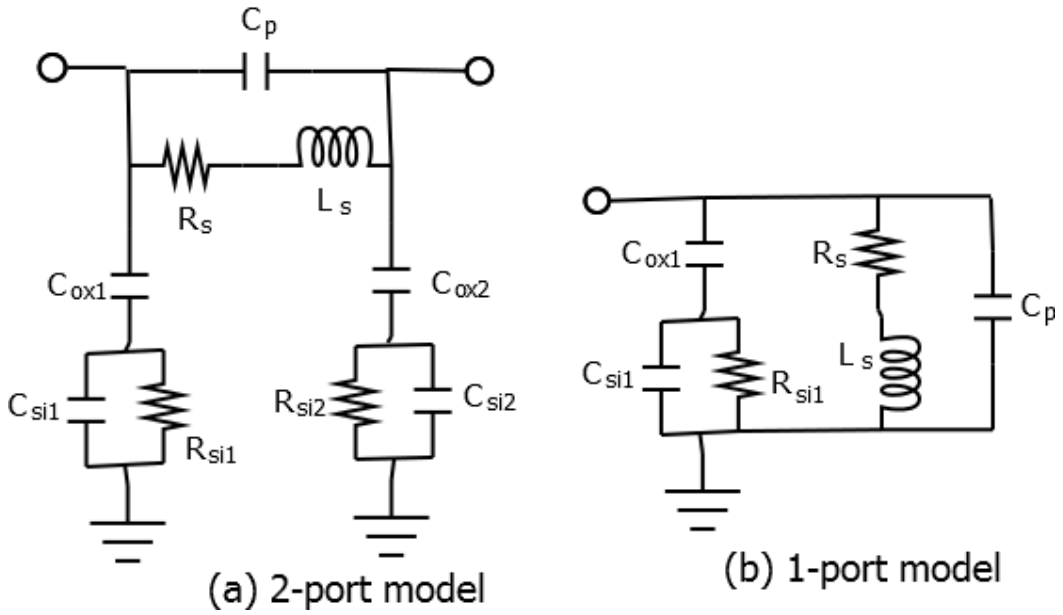

Figure 3.13 Pi-model equivalent circuits of a spiral inductor.

The relevant parameters of the pi-model spiral inductor with silicon substrate are given as follows:

- The parasitic capacitance between the metal tracks (Cp). It does not affect much the inductance value.
- The series inductance of the metal (Ls).
- The series resistance (Rs) of the metal. It includes the eddy current losses and DC resistance of the metal.
- The oxide capacitances (Cox1 and Cox2) which is the coupling capacitance between the substrate and the metal layer.
- The substrate capacitances (Csi1 and Csi2) resulting from the potential differences inside the substrate.
- The substrate resistances (Rsi1 and Rsi2) due to the eddy current losses and the resistivity of the substrate.

The pi-model is used in our design.

3.3.2 Transformer Model

The transformer model is emanated from the pi-model. It includes the magnetic coupling between the substrate and the metal layer. Therefore, the induced magnetic field in the substrate can be controlled more accurately. Figure 3.14 shows the circuit representation of a transformer model spiral inductor.

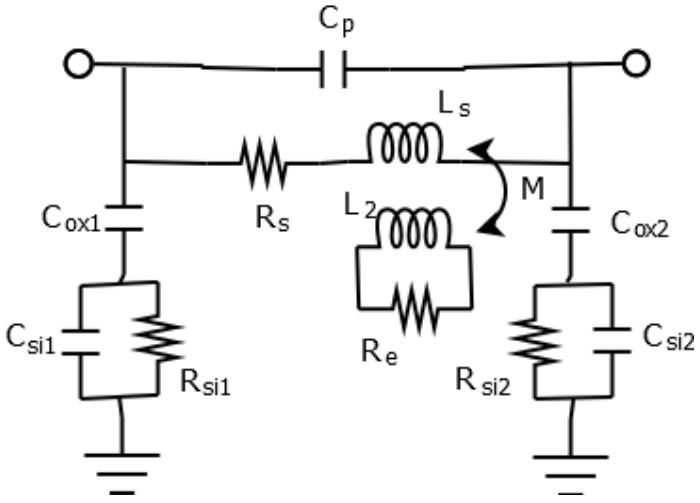

Figure 3.14 Transformer model of silicon substrate spiral inductor.

Additionally, the transformer model has the following parameters:

- The mutual inductance between the substrate and the metal layer denoted by M.
- The resistance due to the eddy current formation in the substrate (R_e).
- The inductance due to the magnetic field induced in the substrate denoted by L_2.

3.3.3 Wideband pi-model

The wideband pi-model is used for wider frequency applications as the its pi-model and transformer model counterparts are best at narrow bandwidth applications. Its circuit representation is given in Figure 3.15.

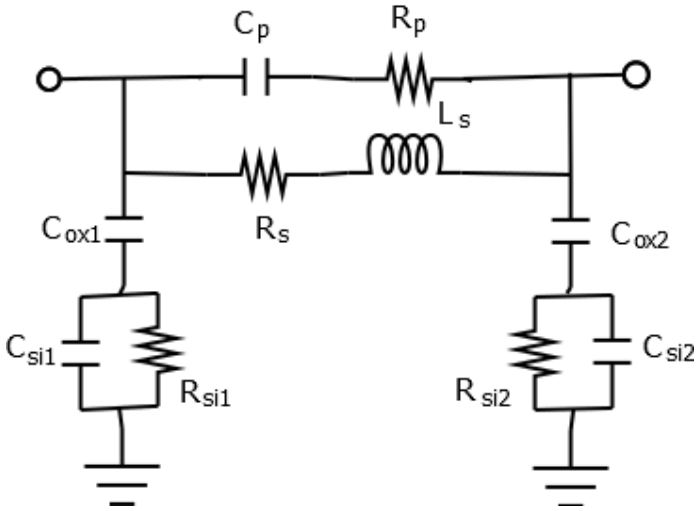

Figure 3.15 Circuit representation of wideband spiral inductor model.

In this chapter, we have presented a descriptive study of a silicon substrate spiral inductor. In the next chapter, we will define the quality factor and present different optimization techniques.

CHAPTER 4

QUALITY FACTOR AND OPTIMIZATION TECHNIQUES OF SILICON SUBSTRATE SPIRAL INDUCTORS

4.1 DEFINITIONS OF QUALITY FACTOR

The definition of the Q-factor depends on the structure in question. For instance, the Q-factor of a transformer is not defined exactly in the same way as that of an inductor. Nevertheless, the Q-factor in general is defined as the ratio of the stored energy to the dissipated energy. It is analogous to the signal to noise ratio in RF devices. In this section, we will define two types of Q-factors that are used when evaluating the performance of integrated inductors: Q_{em} and Q_c.

4.1.1 Q-factor Q_{em}

The Q-factor Q_{em} is a measure of the maximum energy that the inductor can store with respect to the energy loss through its operation in one cycle. It is given by Eq. (4.1).

$$Q_{em} = \frac{W_m \cdot \omega}{P_d} \tag{4.1}$$

where W_m is the maximum magnetic energy, ω the angular velocity and P_d the power loss or dissipated.

4.1.2 Q-factor Q_c

The Q-factor Q_c uses the extracted Y-parameters (or Z-parameters) of the device in question. Therefore, the Y-parameters are first measured. In an unloaded two-port network, Y_{11} indicates the input admittance, which is used for the quality factor

evaluation.The imaginary part of an admittance is proportional to the stored energy while its real part is proportional to the dissipated energy. Thus, Q_c is the ratio of the input susceptance to the input conductance, as given in Eq. (4.2).

$$Q_c = \frac{\mathrm{Im}(Y_{11})}{\mathrm{Re}(Y_{11})} = \frac{2 \cdot \omega \cdot \left(\bar{W}_m - \bar{W}_e\right)}{P_d} \tag{4.2}$$

Where $\bar{W}_m$ and $\bar{W}_e$ are the average magnetic and electric energy stored, respectively. P_d and ω are the power loss and the angular velocity, respectively.

The stored magnetic energy of an inductor is determined by its inductance value. From Figure 3.13 (b), the series inductance Ls is dominant over all other inductances. Thus, the stored magnetic energy is determined by the series inductance of the metal. Similarly, the electric energy stored in the inductor can be found from its capacitance values. For a spiral inductor, the capacitance of the oxide layer (Cox) is the most important. For that reason, the stored electric energy of an inductor is referred to that stored in its oxide capacitance. The power loss is determined by the resistances such as the series resistance (R_s) and the substrate resistance (R_{si}). From the concept of Q_c, the quality factor improves when the series inductance is large while the oxide capacitance and the series resistance are small.

All the above Q-factors take into account the magnetic power stored, the parasitic power and the dissipated power or power loss. In general, improving the Q-factor of a silicon substrate spiral inductor consists of augmenting the inductance and keeping the parasitic capacitances and resistances as low as possible. However, some challenges can be encountered during these improvements. For example, by reducing the resistivity of the metal, the conductivity increases, so does the magnetic field strength. Therefore, strong eddy current can be induced in the substrate which is parasitic to the inductance value. That is why a tradeoff is required sometimes. Many methods of optimizations have been proposed by scientists. They mainly consist of reducing the eddy current effects or reducing the oxide capacitance or increasing the inductance value. Besides the

reduction in the quality factor, the parasitic capacitances play a very important role in the operating frequency reduction due to the self resonance effect.

4.1.3 Self Resonant Frequency (SRF)

The spiral inductor model is composed of a combination of inductances, capacitances and resistances coming from either the metal or the dielectric substrate, as shown in its equivalent circuit. As a result, the input impedance is composed of a real and an imaginary part. The real part mainly contains the resistance values and it causes power dissipation. On the other hand, the imaginary part is constituted by the inductance and capacitance values and stores magnetic or electric energy. As the inductor is expected to store magnetic energy, an ideal spiral inductor has the highest possible value of inductance and the lowest possible values of capacitance and resistance. Nevertheless, the latter parameters are also frequency dependant. At low frequencies, the inductance value is dominant over all the other parameters. That is why the Q-factor of a spiral inductor is maximal at lower frequencies. As the frequency increases, the resistance value increases due to the skin effect. Similarly, the capacitance increases with frequency due to the proximity effect. As the capacitance increases, it takes part of the energy stored by the inductance which thus starts to decrease. The two impedence values evolve in the opposite direction and eventually equal to each other at a frequency called ***the self resonant frequency*** (SRF). Beyond this frequency, the inductor exhibits a capacitive behavior rather than an inductive one. For a one port network of pi-model spiral inductor as represented in Figure 3.13 (b), the SRF can be expressed in Eq. (4.3):

$$\omega_{SRF} = \frac{1}{\sqrt{L_s C_{ox1}}} \cdot \sqrt{\frac{L_s - R_s^2 C_{ox1}}{L_s - R_{si1}^2 C_{ox1}}} \tag{4.3}$$

Among the parasitic capacitances, the oxide capacitance (C_{ox1}) is the most important. The quality factor of a silicon substrate on-chip inductor is the maximum at a frequency (ω_{Qmax}) lower than the SRF. This frequency is expressed in Eq. (4.4).

$$\omega_{Q\max} = \frac{1}{\sqrt{L_s C_{ox1}}} \cdot \sqrt{\frac{R_s}{2R_{si1}}} \cdot \left[\sqrt{1 + \frac{4R_{si1}}{3R_s}} - 1 \right]^{1/2} \tag{4.4}$$

4.2 CURRENT OPTIMIZATION TECHNIQUES OF INTEGRATED SPIRAL INDUCTORS

There are several Q-factor improvement techniques that are being implemented in order to produce a high quality and high inductance density on-chip inductor that can operate in several gigahertz. Among these techniques, the most important ones are: *N-type layer formation under the oxide layer, substrate shielding, metal stacking, suspending the inductor, magnetic thin film introduction*. We will briefly discuss each technique below.

4.2.1 N-type layer formation

Due to its high dielectric constant, the oxide capacitance of a spiral inductor is relatively large. Thus, the quality factor and SRF are poor. To reduce the oxide capacitance, one way is to form an N-type layer below the oxide layer, as shown in Figure 4.1. A DC bias is applied to this N-layer to form a depletion layer. The depletion layer will have a relatively small capacitance (C_d) that will be in series with the capacitance of the oxide layer. The total capacitance is therefore reduced.

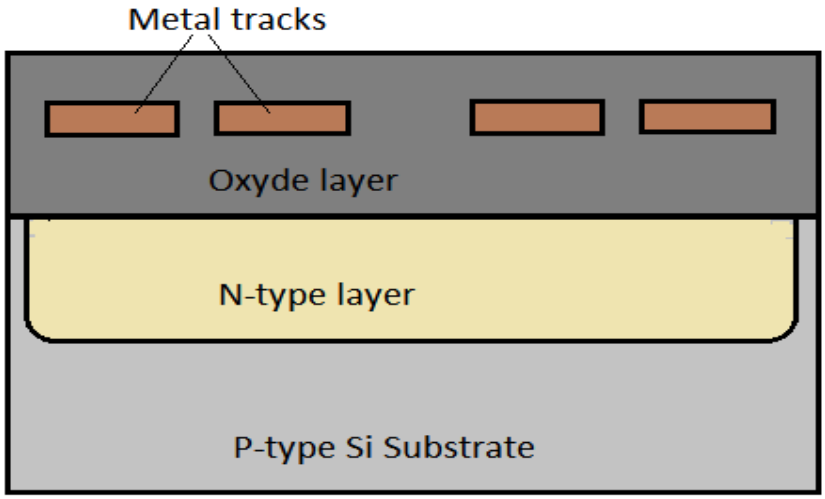

Figure 4.1 N-type layer under the oxide of an inductor.

The equivalent circuit of Figure 4.1 is given in Figure 4.2. From Figure 4.2, the energy dissipated can be computed using Eq. (4.5).

$$E_d = \frac{V^2}{\mathrm{Re}(Z_T)} \tag{4.5}$$

where E_d represents the energy or power dissipated, V the applied voltage and Z_T the total impedance of the inductor.

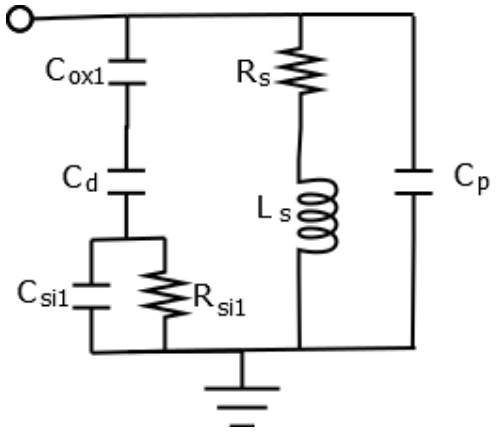

Figure 4.2 Equivalent circuit of a spiral inductor with N-type layer under the oxide layer.

The total impedance Z_T is calculated using Eq. (4.6).

$$Z_T = jX_{C_p} \square \left(R_s + jX_{L_s}\right) \square \left(jX + R_{si1} \square jX_{C_{si1}}\right) \tag{4.6}$$

where X_{Cp}, X_{Ls}, X_{Csi1} are the reactances of the capacitor C_p, the inductance L_s and the capacitor C_{si1}, respectively. X is the equivalent reactance of the series connection of capacitance C_d and C_{ox1}.

After calculating the total impedance and taking its approximate real part, Eq. (4.5) becomes as follows:

$$E_d = \frac{V^2}{X^2 + R_{si1}^{\ 2}} R_{si1} \tag{4.7}$$

Since X is the series reactance of C_{ox1} and C_d, it decreases as expressed in Eq. (4.8).

$$X = \frac{C_{ox1} + C_d}{C_{ox1} \cdot C_d} \cdot \frac{1}{\omega} \tag{4.8}$$

This value of X is increased due to the effect of C_d combined with C_{ox1} resulting in a lower value of energy loss. Therefore, the quality factor is boosted.

4.2.2 Substrate shielding

Since the silicon substrate is usually too lossy, the idea of cancelling its effect emerged with the shielding technique. This technique consists of placing a material shield under the spiral of the silicon substrate inductor, as given in Figure 4.3. Materials such as polysilicon are preferred as shielding materials due to their high conductivity. The oxide and substrate are therefore replaced by a shield with resistance R_{sh}. There exists a capacitance between the substrate and the shield denoted by C_{sh}. In addition, the shield must be slotted in order to avoid current circulation, which could form a negative mutual inductance. These slots should be small to avoid the penetration of electric field into the substrate.

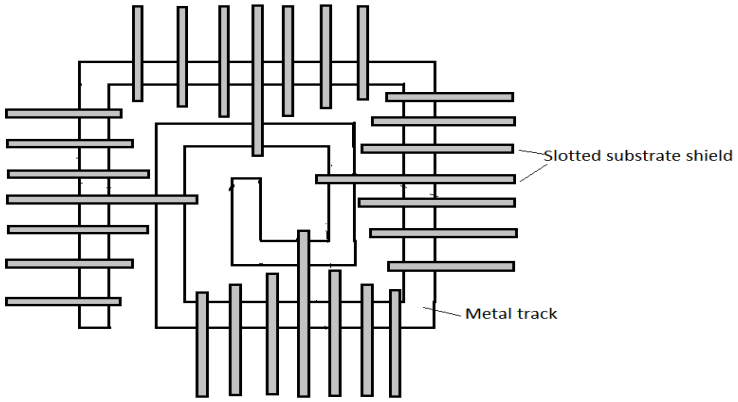

Figure 4.3 Shielded substrate spiral inductor

The equivalent circuit of a spiral inductor with substrate shield is given in Figure 4.4.

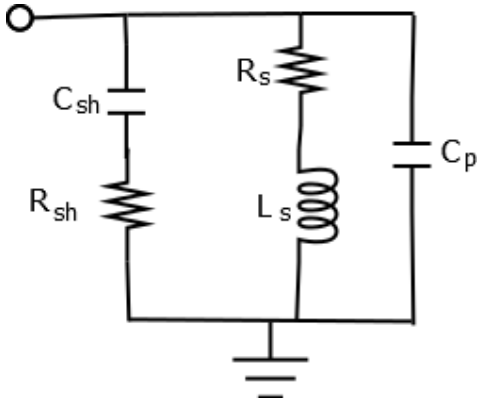

Figure 4.4 Equivalent circuit of a spiral inductor with shielded substrate.

The energy loss equation can be written as follows:

$$E_d = \frac{V^2}{\left(\frac{1}{\omega C_{sh}}\right)^2 + R_{sh}^{\ 2}} R_{sh} \tag{4.9}$$

where R_{sh} and C_{sh} are the resistance and capacitance of the substrate shield, respectively.

Since the resistivity of the substrate shield is much smaller than that of the silicon substrate, the dissipated energy is reduced for a specific range of frequency. Therefore, a significant quality factor improvement can be observed in that range. However, the shield capacitance (C_{sh}) is larger than the oxide capacitance. Thus, the self resonant frequency is decreased, limiting the frequency range of operation.

4.2.3 Stacking of metal layers

As stated before, by increasing the metal width, the resistance can be lowered. This can be also achieved by stacking several metal layers and connecting them through

vias, as shown in Figure 4.5. Stacking the metal layers can also increase the inductance density to a very high value.

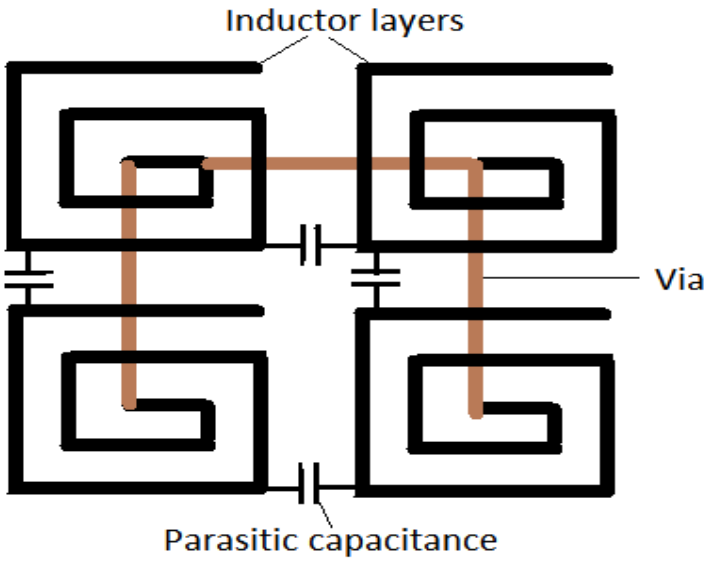

Figure 4.5 Stacked spiral inductor layers.

Stacking inductor layers is a very efficient method in improving the inductance density of a spiral inductor. On the other hand, there are parasitic capacitances between these layers which cut off the frequency range of the inductor. However, the quality factor improvement is still good in several gigahertz.

4.2.4 Suspended inductors

If the lossy nature of the substrate is the main source of quality factor deterioration, why not remove it? Indeed, the silicon substrate is crucial for the integration purpose since almost all the CMOS process circuits are built on a silicon substrate. That is why they cannot be totally removed. However, their contact with the inductor can be decreased by suspending the latter. One way of suspending an inductor is to used plating deformation magnetic assembly (PDMA), as shown in Figure 4.6.

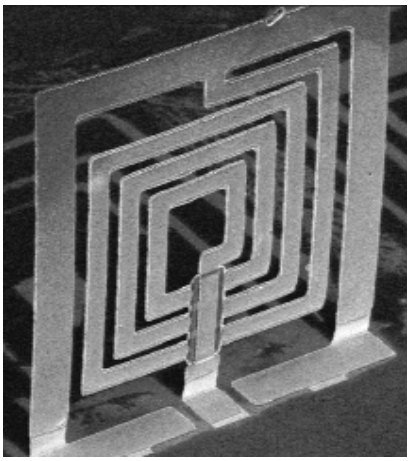

Figure 4.6 Suspended inductor using PDMA method.

The plating deformation magnetic assembly consists of depositing the spiral metal on a sacrificial layer, beneath which is located the substrate. Later, the sacrificial layer is removed. One side of the inductor should be fixed to the substrate. An external magnetic field is then applied to the structure to vertically lift the inductor as shown in Figure 4.6.

The advantages of using this method are the elimination of substrate effects and reduction of the footprint of the inductor.

4.2.5 Introduction of magnetic core in spiral inductors

Magnetic thin films such as ferrite films have high magnetic permeability. Depositing these films under or above the metal layer, as shown in Figure 4.6, can therefore increase the inductance value of the spiral inductor. The magnetic material properties should be adequate with the gigahertz applications.

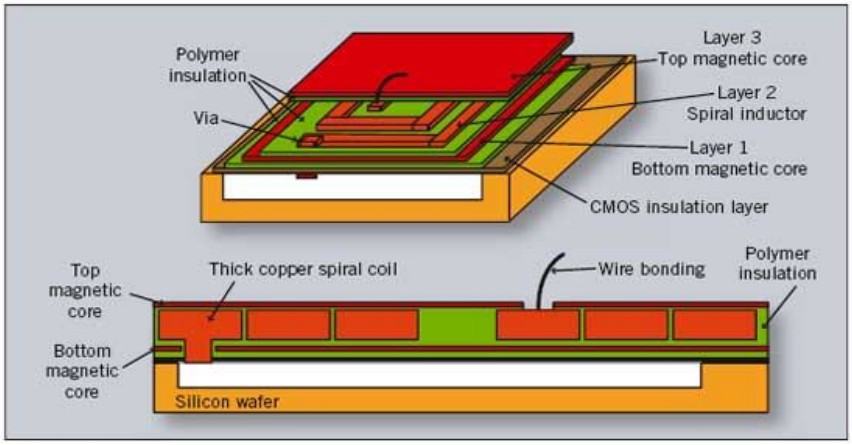

Figure 4.7 Spiral inductor using magnetic core.

The use of magnetic core beneath, or above the spiral of an inductor causes very crucial inductance value improvement. The quality factor can be improved up to a certain frequency value (e.g. 2 GHz). However, at higher frequencies, the hysteresis and eddy current losses become very important due to the high conductivity of ferromagnetic materials, thus the quality factor decreases exponentially. Another effect that limits the frequency range of these types of inductor is the ferromagnetic resonance (FMR) which causes energy dissipation in the inductor. Beyond the frequency at which the FMR occurs, the magnetic core draws a diamagnetic behavior, meaning it becomes useless.

As mentioned before, FM materials play a very important role in increasing the inductance density of an on-chip spiral inductor. However, using FM materials encounters drawbacks such as hysteresis and eddy current losses as well as FMR effect. Therefore, we have elaborated a new idea that implies the usage of the mixture of FM materials and polymer to form a semi magnetic core that exhibits some magnetic characteristics with moderate losses.

In the next chapter, we will present our proposed design methodology, the simulation results using the HFSS software program and the fabrication process.

CHAPTER 5

DESIGN OF INDUCTORS USING POLYMERS AND FERROMAGNETIC MATERIALS

5.1 FERROMAGNETIC MATERIALS

Magnetic materials are widely used in telecommunications from transformer to inductor designs. Trade offs between the size, the cost and the performance are made in general in the designs involving magnetic materials. Magnetic materials can be classified as diamagnetic with permeability less than 1, paramagnetic with permeability greater than or equal to unity and ferromagnetic with permeability much greater than unity. Ferromagnetic materials are preferred when it comes to inductor design. They include iron, silicon steel, nickel, iron, ferrites, etc.… Every magnetic material is characterized by its magnetization curve (see Figure 5.1). Five main properties can be deduced from this curve: ***Permeability*** μ, ***saturation field strenght*** Bs, ***resistivity*** ρ of the core, ***remanence*** Br and ***Coercivity*** Hc.

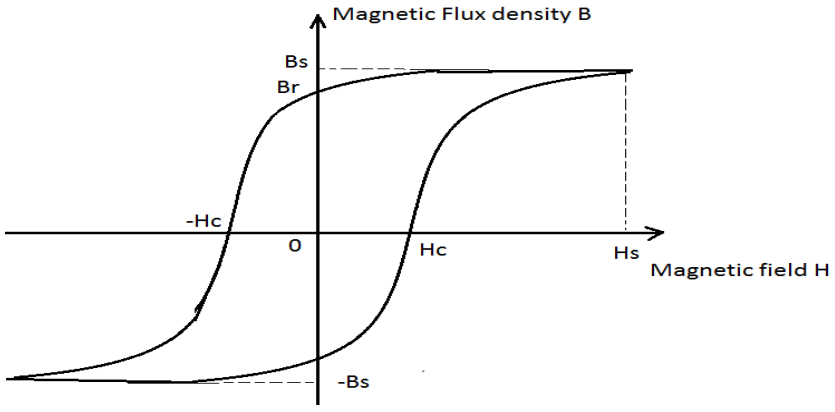

Figure 5.1 Magnetization curve of magnetic materials

5.1.1 Magnetic permeability

The magnetic permeability (μ) is a crucial parameter that determines how good a magnetic material is. It is formulated by taking the ratio of the flux density B to the field strength H, as expressed in Eq. (5.1)

$$\mu = \frac{B}{H} \tag{5.1}$$

As we can understand from the B-H curve in Figure 5.1, the permeability does not have a linear relation with respect to the field H. It has a normal distribution alike curve, which is represented in Figure 5.2

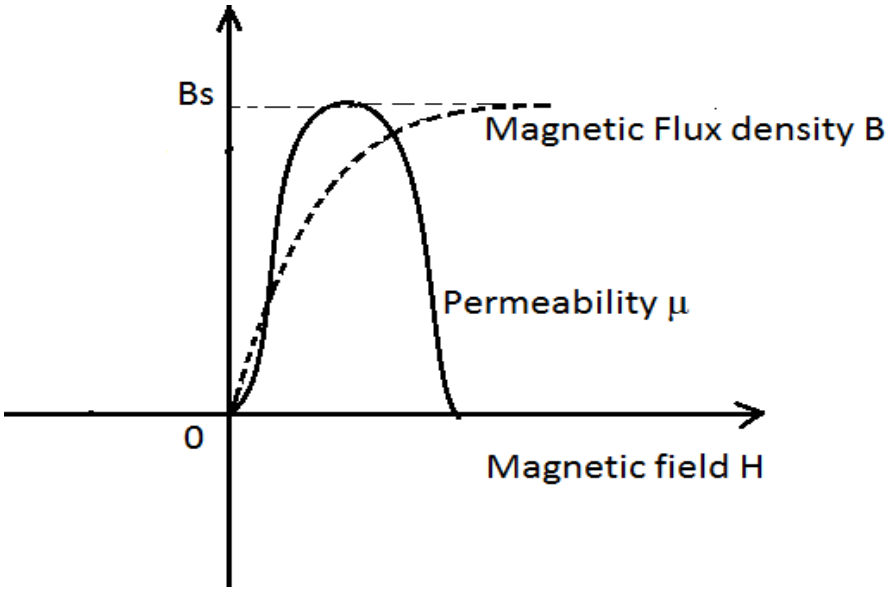

Figure 5.2 Graph of magnetic permeability with respect to field strength H.

Magnetic susceptibility (χ) is usually used to analyze the magnetic properties of a material. It is indeed related to the magnetic permeability, as given in Eq. (5.2).

$$\mu = \mu_0 (1 + \chi) = \mu_0 \mu_r \tag{5.2}$$

where μ_0 is the permeability of free space and μ_r is the relative permeability.

The higher the magnetic susceptibility, the better the magnetic material. Just like the permeability, the susceptibility characterizes all magnetic materials. At low frequencies, the susceptibility is a real value and increases with the applied field. At high frequencies (e.g. Gigahertz frequencies), the electrons in the magnetic core fail to keep up with alternating field. This difference in alternation between the electrons and the applied field creates some stored energy as well as some core losses. Therefore, the susceptibility becomes a complex value, formulated in Eq. (5.3).

$$\chi(\omega) = \chi'(\omega) - j\chi''(\omega) \tag{5.3}$$

In fact, it is wished that the real susceptibility (χ') is high while the imaginary susceptibility (χ'') is low, because the former stored magnetic energy and the latter produces core losses.

The complex susceptibility is also frequency dependant. As the frequency increases, its real and imaginary parts increase simultaneously and reach their peaks before decreasing. The frequency at which the imaginary part of the susceptibility reaches its peak is called ***Ferromagnetic resonance (FMR) frequency***, and is depicted in Figure 5.3. This frequency roughly cuts the operating frequency range of inductors using FM materials. After the FMR frequency, the FM core becomes paramagnetic.

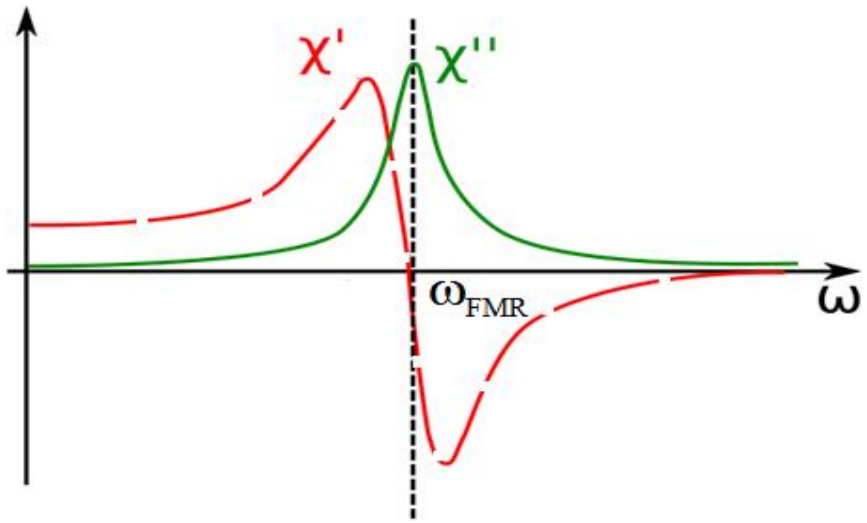

Figure 5.3 Ferromagnetic resonance.

The FMR frequency is expressed in Eq. (5.4).

$$\omega_{FMR} \cong \gamma \sqrt{H_k \left(H_k + 4\pi M_s \right)} \tag{5.4}$$

where γ is the gyromagnetic ratio, H_k the anisotropy magnetic field, and Ms is the saturation magnetization.

We can observe from Eq. (5.4) that the FMR frequency is related to the saturation magnetization or magnetic flux density and the anisotropy effect in the material. The higher these parameters, the higher the FMR frequency and the better the magnetic core. The anisotropy effect in FM material is the fact that the magnetization under a certain magnetic field value follows an easier pattern instead of the usual one. This is due to several effects: Crystal orientation of the atoms, the orientation preference of the grains, presence of pores, temperature, etc.…

5.1.2 Saturation

As shown in the magnetization curve in Figure 5.1, a gradual increase in the magnetic field strength leads to a point where the flux density does no more increase significantly. This point is the saturation. The magnetic field that is necessary to reach the saturation is denoted by H_s, while the corresponding flux density is represented by B_s. In order to have a better magnetic behavior, a magnetic material must have a high saturation flux density.

5.1.3 Remanence flux and Coercivity

When a magnetic material is gradually excited by a field H, the flux density increases and reaches a saturation point. When the excitation is gradually decreased after the saturation point, the curve follows a different pattern than its previous one. This pattern is above the previous one and is due to the magnetization effect. The material after being magnetized stored some energy that remains even after annulling all excitations. The remaining flux in the magnetic core after reducing the excitation to zero is called the ***Remanence flux density or retentivity*** and denoted by Br. By further decreasing the magnetic field excitation after the zero level, we will reach a point where the flux density equals to zero. The applied field corresponding to this point is called

Coercivity. In another word, the coercivity is the amount of negative magnetic field necessary to bring the remaining flux to zero. The magnetic material can be defined to be either magnetically soft or hard depending on whether it has a low or high coercivity. Magnetically soft materials or materials having low coercivity are desired in the inductor application due to their low loss generation.

5.1.4 Hysteresis and core losses

During the magnetization process, the magnetic supply delivers an amount of power to the magnetic material. After reaching the saturation, by gradually decreasing the applied field, the material is thus exposed to a process of demagnetization. In clear, the previously delivered power is being driven back to the supply. However, instead of following the same curve of the magnetization, the demagnetization curve follows a path that is above the positive excitation curve as shown in Figure 5.1. The area between the magnetization curve and the B–axis determines the energy or power delivered to the material. Similarly, the energy returned back to the supply is represented by the area between the demagnetization curve and the B – axis. Considering these hypotheses, we can clearly observe that the energy supplied is greater than that returned. That means there has been an amount of energy lost throughout the core called ***hysteresis loss***. The hysteresis loss translates into heat and is determined by the area of magnetization loop or hysteresis loop. On the other hand, the ***eddy loss*** is due to the induced current in the material emanating from the e.m.f produced by the magnetic field applied. Further, the eddy loss is related to the ***resistivity*** ρ of the conductor. The higher the resistivity, the lower the eddy loss. As we have previously mentioned, a magnetic field produces eddy current loops in any conducting material interfering it. In the application of on-chip spiral inductors, the FM material should have a hysteresis loop as narrow as possible.

All the above properties are important in choosing the type of FM core to be used in the design of a spiral inductor. Basically, it will be ideal to have a material that has:

(a) High saturation flux density or magnetization;
(b) High magnetic permeability with reduced reactive susceptibility;
(c) Narrow magnetization loop and high resistivity.

Although FM materials have naturally high value of permeability as shown in Table 5.3, it is impossible to have a simple FM material that exhibits all the above requirements at the same time. For example, the materials that have narrow magnetization loops, known as magnetically soft material as mentioned before, have relatively lower values of saturation flux density in general. For that reason, one needs to do a trade off between in a way to fulfill his or her demands. For instance, if we consider using FM core in the spiral inductor, we are more concerned about getting a high value of μ at higher frequencies and high resistivity.

Table 5.1 Properties of different FM materials

Metal	Relative Permeability	Conductivity (Ω.m)
Permalloy	8000	0.22×10^7
Iron	5000	1.43×10^7
Nickel	600	1.43×10^7
Cobalt	250	0.18×10^7

The ferromagnetic materials have high permeability and low resistivity. Using them under the metal layer of the ordinary spiral inductor results into the production of high self inductance value. However, the quality factor drops due the significant amount of negative mutual inductance. Another issue with the FM materials is the low FMR frequency which limits the frequency range of operation of an inductor. Therefore, a novel material which produces high self inductance and low negative mutual coupling as well as relatively higher operating frequency range is preferred and will be studied in the next section.

5.2 MIXTURE OF POLYMERS AND FM MATERIALS

Polymers are practically insulators but have very low permeability. On the other hand, FM materials such as iron have very high permeability but very conductive with low FMR frequencies. As we have stated in the previous section, it is usually not preferred to use FM materials only in the inductor design. Nevertheless, by mixing a polymer and FM nanoparticles, it is possible to obtain a core that has high resistivity and high permeability at the same time. However, real measurements are required to depict the most approximate values of the resistivity and the permeability. After the measurements of the inductors, we can extract the approximate values for the relative permeability and permittivity of the novel core.

Since our improvement method necessitates the use of polymers, the selection criteria of the appropriate polymer is a matter of study. Hence the next section is dedicated to a shot study of the polymers that can be possibly used in our design.

5.3 POLYMERS

A Polymer is a material composed of one or many substances connected in chains. They are actively employed in nanofabrication of RF and CMOS devices due to their multiple applications. Polymers can be used as dielectrics, insulators or protective layers (e.g. Polyimides). They are also used as masking layers in Lithography process (e.g. photoresist) and deposition processes such as electroplating. Some polymers are very resistant and allow the deposition of very thick layers without any damage. These are called ***High Aspect Ratio*** (HAR) polymers. The deposition of a thick metal layer is important for reducing the electric resistance at low frequencies. One example of HAR polymers is SU-8. SU-8 is a negative photoresist composed of epoxy resin that operates at wavelengths close to the UV. Therefore, it is not very light sensitive, allowing thicker layer deposition. Other HAR polymers include PMMA and AZ4562 (see Table 5.1).

Table 5.2 Comparison of HAR polymers

Resist	PMMA	SU-8	AZ4562
Exposure type	X-ray (0.2-2 nm)	UV (365, 405, 435 nm)	UV (365, 405, 435 nm)
Light source	Synchrotron facility	Mercury lamp	Mercury lamp
Mask substrate	Beryllium (100 μm) Titanium (2 μm)	Glass (1.5-3 mm) Quartz (1.5-3 mm)	Glass (1.5-3 nm) Quartz (1.5-3 mm)
Mask absorber	Gold (10-15 μm)	Chromium (0.5 μm)	Chromium (0.5 μm)
Maximum height	1000 μm	250 μm	100 μm
Aspect Ratio	500	20-25	10
Young's Modulus (GPa)	2-3	4-5	-
Poisson's ratio	-	0.22	-
Glass Temperature (Celsius)	100	>200	-

Polymers in general are insulators therefore do not allow electrical conduction. Thus, using them in integrated spiral inductors, one can take the advantage of reduced eddy current production.

As seen from Table 5.1, SU-8 is compatible with glass and quartz substrates up to 3mm. It can be processed with UV light which makes it cheaper compared to PMMA. Besides, it can be used as a structural layer with a very high aspect ratio, hence excluding the need of AZ4562 in most applications. Because of this flexibility, we are using SU-8 in our design. Table 5.2 shows the electrical properties of SU-8 photoresist.

Table 5.3 Properties of SU-8

Property	Value
Breakdown voltage	$\geq 1.1\times10^{5} V/m$
Relative dielectric constant ε_r	4.2 (at 10GHz), 4 (20 GHz - 40 GHz)
Volume resistivity	$1.8-2.8\times10^{16}\Omega\cdot cm$
Magnetic permeability μ_r	1.08
Refractive index	1.575 – 1.8
Absorption coefficient α	2 – 40 cm^{-1}
Loss tangent	0.08 – 0.14

5.4 METHOD AND FABRICATION

5.4.1 Method and Software Optimization

Our aim of this project is to show the inductance density and the quality factor improvement due to the use of a novel material –which is FM-polymer core in the spiral inductor. The HFSS simulation software was used for simulation and optimization purposes. It is important to always use a simulation software before starting any real fabrication. By sweeping the parameters, it is possible to have optimum results at the desired frequency. Using the HFSS software, a 1 nH and a 5 nH inductors were designed and simulated. These inductors were designed with a glass substrate, a polymer (SU-8) on top of the substrate and a circular spiral copper pattern inside the SU-8 layer. In addition, these inductors were optimized by using parameterization to get the minimum sizes. However, our optimization is limited by the capability of the available facility which allows a minimum width of 10 μm. Therefore, all the sizes must be above that value. The Inductance values and Q-factors of these inductors were plotted with respect to frequency in a rectangular graph. Our frequency of interest is 7.95 GHz. The Q-factor was plotted by using Eq. 4.2. The inductance was determined by taking the imaginary part of the input impedance (Z_{11} or $1/Y_{11}$) and dividing by two pi times the frequency (f) as given in Eq. 5.1. Note that this equation only gives an approximate value of the inductance since it ignores the parasitic capacitance values.

$$L_s = \frac{\mathrm{Im}(Z_{11})}{2\pi \mathrm{f}} \tag{5.1}$$

Later, the 1 nH and 5 nH inductors were re-designed and simulated by replacing the SU-8 with the FM-SU8 core that has a relative permeability assumed to be 10. The inductance value and Q-factor of these new inductors were plotted and compared to the previous results. Lastly, the microfabrication process in the clean room was started, but not terminated in the time frame. However, the simulation results are sufficient to observe the improvement factors.

5.4.2 Fabrication process

After the software optimization, comes the fabrication process which involves fabrication devices and the clean room. A soft baked glass substrate is used as the

basement. Photolithography is then used on the photoresist coated substrate. Next, we deposit a thin copper layer uniformly using Sputtering process. Lift-off is used to vanish away the copper non-located on the spiral pattern. Then, we coat the surface with a thick SU-8 polymer or the SU8-FM mixing core layer by using spin coating. Next, the exposure is started in the photolithography process. After development, the SU-8 on top of the metal pattern is removed. Later, Electroless plating is applied to deposit the copper layer on the spiral metal pattern to level it to the core. A thicker metal layer can be deposited since SU-8 is a HAR polymer. The overpass is formed after we finish with the two-dimensional fabrication. Lastly, metallization is used to make metal contacts for the real measurement purpose. Figure 6.1 depicts the summarized microfabrication process of the inductors.

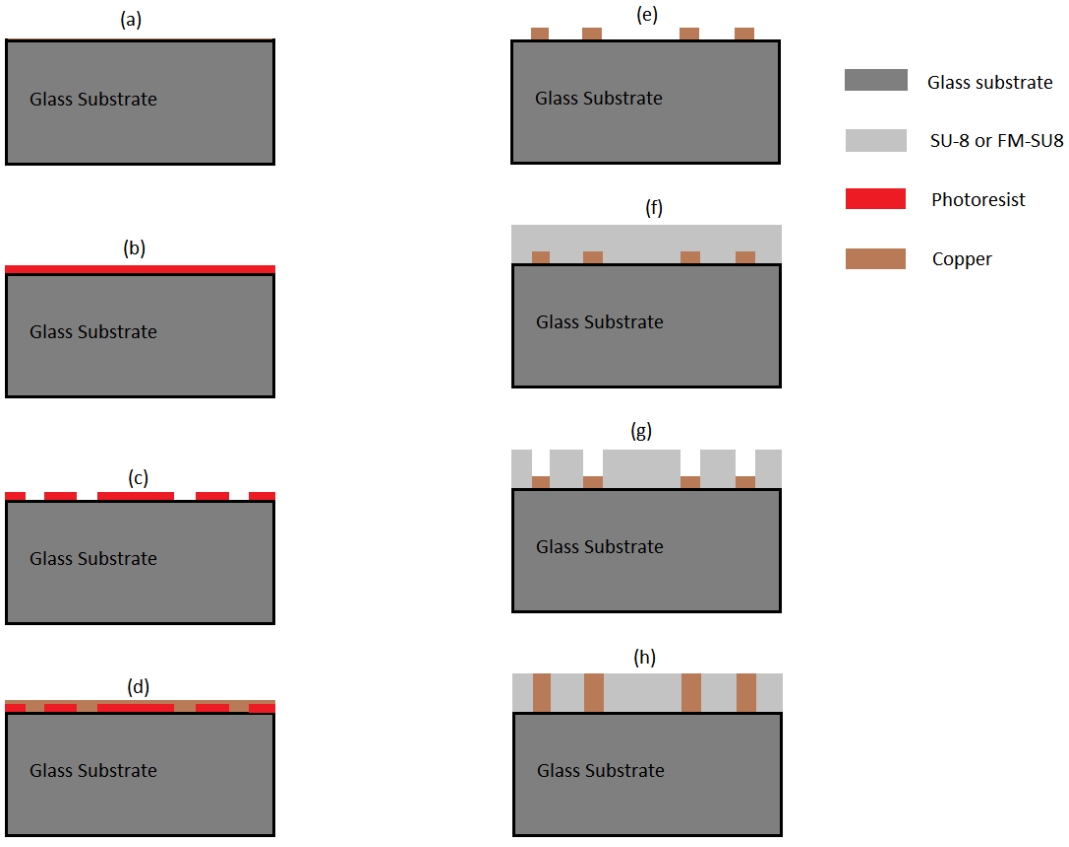

Figure 5.4 Fabrication steps of a spiral inductor using SU8-FM core.

CHAPTER 6

RESULTS AND DISCUSSION

In this project, we have assumed the permeability of the FM-SU8 core to be 10.

Table 6.1 shows the design parameters for the 1 nH and 5 nH with and without the FM-SU8 core after simulations.

Table 6.1 Design parameters of inductors using SU-8 and SU8-FM cores.

	1 nH with SU8 core	1.6 nH with SU8-FM core	5 nH with SU8 core	5 nH with SU8-FM core
Internal radius ri (in μm)	25	10	98	48
Metal width Wm (in μm)	10	10	10	10
Metal thickness Tm (in μm)	10	10	10	10
Turn number N	2.97	2.97	2.97	2.97
Spacing between coils S (in μm)	10	10	20	20
Side length of the inductor l (in μm)	179	148	325	284

Comments: we can observe a decrease in the size of the inductors when we use the FM-SU8 core in both cases.

The Simulation results are presented in Figure 6.1 (a) and (b).

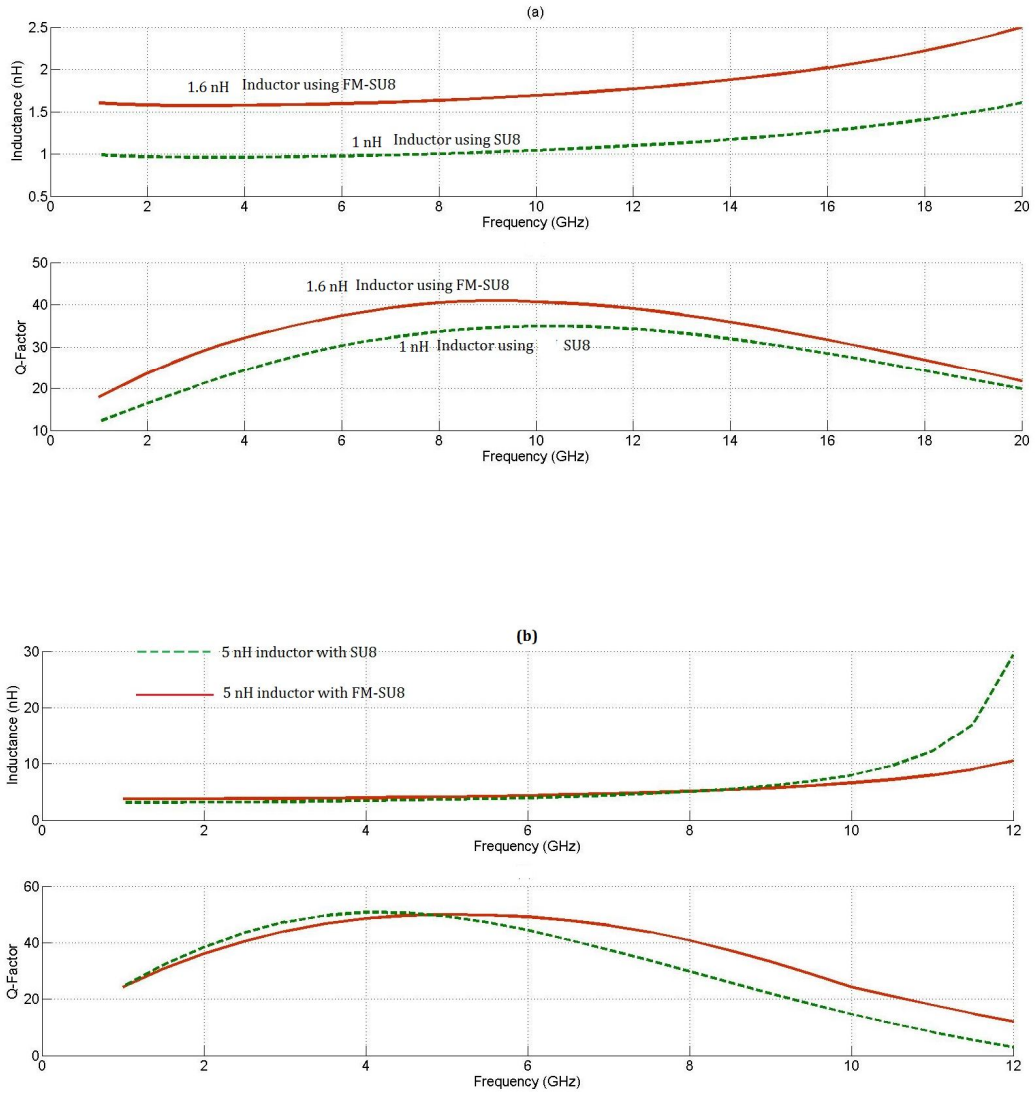

Figure 6.1 Comparison between the inductors using SU-8 and the inductors using FM-SU8. (a) 1.6 nH inductor with FM-SU8 versus 1 nH inductor with SU8 at 7.95 GHz. (b) 5 nH inductor with FM-SU8 versus 5 nH inductor with SU8 at 7.95 GHz.

From Figure 6.1, we can say that the Q-factor was improved from 34 to 40 for the 1.6 nH inductor and from 30 to 41 for the 5 nH inductor when we use FM-SU8 core.

Table 6.2 summarizes the results

Table 6.2 Comparison between inductors using SU-8 and SU8-FM cores.

	1 nH with SU8 core	1.6 nH with SU8-FM core	5 nH with SU8 core	5 nH with SU8-FM core
Length of the inductor (μm)	178	148	376	284
Q-Factor	34	40	30	41

Figure 6.2 represents the progressive picture of the inductor during Fabrication. The de-embedding measurement technique can be used since the measurement probes are relatively large. It consists of measuring the chip with the metal contacts and measuring the metal contacts only then subtracting the measurement values of the metal contacts from that of the chip.

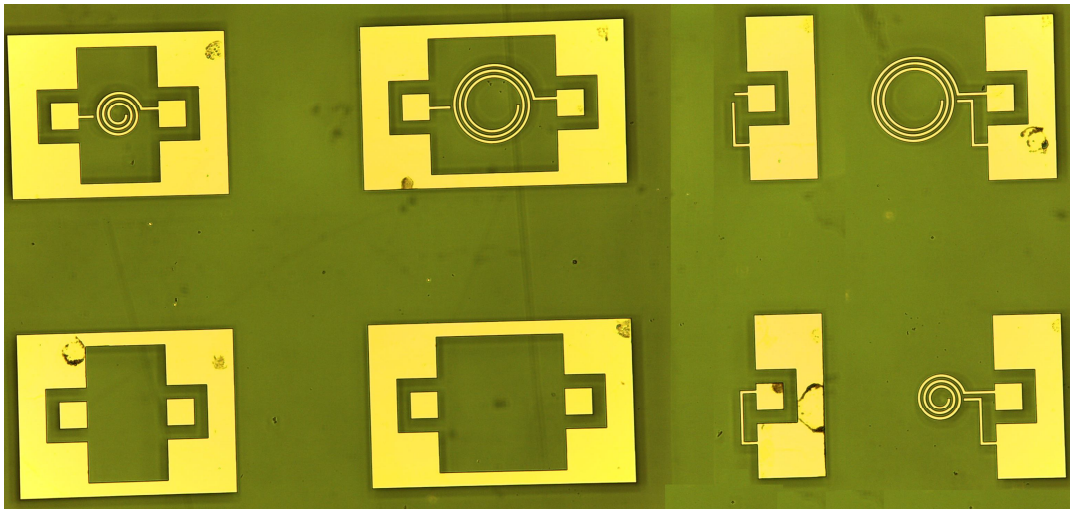

Figure 6.2 Fabricated inductors (in progress) and metal contacts

CHAPTER 7

CONCLUSION

In this study, we have first highlighted the importance of high Q-factor inductors used in on-chip applications. All devices for receiving and transmitting as well as amplification contain inductors. Next, we have presented a descriptive study of integrated spiral inductors using a silicon substrate with different loss mechanism associated with its operation. Basically, a simple spiral inductor is composed of spiral metal tracks that can be in polygonal or circular shape, a dielectric material (e.g. Silicon dioxide) and a silicon substrate at the bottom. Due to the conductivities or resistivities of the metal and the semiconductors, spiral inductors exhibit losses that are either electrically induced or magnetically induced. Because of these losses, the Q-factors of integrated spiral inductors are poor in general. Later, we have studied different quality improvement techniques that are being used along with their drawbacks. Techniques such as ground shielding and stacking of metal layers are very common. However, they encounter the problem of reduced self resonant frequency which limits the operating frequency range of the inductor. Lastly, we have proposed a novel method that implies the use of a mixture composed of a polymer (SU-8) and an FM material. This mixture is an insulating material that exhibits some magnetic properties. Using HFSS software, we have presented the inductance and Q-factor simulation results of two different inductors (1 nH and 5 nH) using SU-8 core with the minimum possible sizes. The frequency of interest was 7.95 GHz. Then, we have replaced the SU-8 by the FM-SU8 core and repeated the simulations for the minimum sizes obtained. Taking into account the limitations of the available facilities, we managed to design a 1.6 nH and a 5 nH inductors that use FM-SU8 core that has a permeability of 10. For the 5 nH inductor, we observed a reduction of size of 24%, while the Q-factor was improved by 36%. The size of the 1.6 nH inductor with FM-SU8 is 1.2 times less than that of the 1 nH inductor with

SU8; and the quality factor improvement is 20%. We can conclude that the performance of the inductor is improved when we use a mixture of an insulating polymer (SU8) and an FM material in the trench of a spiral inductor. Although the fabrication process was not completely finished, the simulation results proved to be sufficient to observe the improvement factor of our new magnetic material.

The use of Polymer-Ferromagnetic mixture in future ICs can have significant advantages. The quality factors of different elements like transistors and capacitors can be further improved. At the same time, an important improvement in their sizes can be observed. Therfore, we can improve the performances of devices such as cellphones, computers by keeping their sizes even smaller.

REFERENCES

[1] M. Parisot, Y. Archamnault, D. Pavlidis, J. Magarshack, *Highly accurate design of Spiral Inductors for MMIC's with Small Size and High Cut-off Frequency Characteristics.*

[2] K. Araki, H. Ueda, M. Takahashi, *Electronics Letters* 28th March 1985 Vol. 21 No. 7.

[3] C. Patrick Yue, Changsup Ryu, Jack Lau, and S.Simon Wong, *A Physical Model for Planar Spiral Inductors on Silicon*.

[4] Joachim N. Burghartz, *Fellow, IEEE*, and Behzad Rejaei, *On the design of RF Spiral Inductors on Silicon*.

[5] C. Patrick Yue, *student member, IEEE*, and S. Simon Wong, *Senior member, IEEE*, *On-Chip Spiral Inductors with Patterned Ground Shields for Si-Based RF IC's.*

[6] Xiangming Xu, *Member, IEEE*, Pingliang Li, Miao Cai, and Bo Han, *Design of Novel High- Q-Factor Multipath Stacked On-Chip Spiral Inductors.*

[7] J. Zhan, C. Yang, X. Wang, Q. Fang, Z.T. Shi, Y. Yang, T.-L. Ren, A. Wang Y.H. Cheng, L.-T. Liu, *Stacked-spiral RF inductors with vertical nanoparticle magnetic core for radio-frequency integrated circuits in CMOS*.

[8] James Aguilera and Rock Berenguer, *Design and Test of Integrated Inductors for RF Applications*, 2004.

[9] Colonel Wm., T. McLyman, *Transformer and inductor design handbook,* 3rd edition, Revised and Expanded, Kg Magnetics inc. Idyllwild, California, U.S.A.

[10] Jonathan Rosenfeld, *On-Chip Resonance in Nanoscale Integrated Circuits*, University of Rochester, New York, 2009.

[11] Ji Chen, *On-chip Spiral Inductor/Transformer Design and Modeling for RF Applications*, University of Central Florida, Orlando, Florida, 2006.